



KUNGL  
TEKNISKA  
HÖGSKOLAN

# Non-reflecting Boundary Conditions for Wave Propagation Problems

Daniel Appelö

Stockholm 2003

Licenciate's Thesis  
Royal Institute of Technology  
Department of Numerical Analysis and Computer Science

Akademisk avhandling som med tillstånd av Kungl Tekniska Högskolan framlägges till offentlig granskning för avläggande av teknisk licentiat-examen fredagen den 12 december 2003 kl 10.00 i sal D31, Huvudbyggnaden, Kungl Tekniska Högskolan, Lindstedtsv 17 , Stockholm.

ISBN 91-7283-628-8

TRITA-NA-0326

ISSN 0348-2952

ISRN KTH/NA/R--03/26--SE

© Daniel Appelö, December 2003

Högskoletryckeriet, Stockholm 2003

## Abstract

We consider two aspects of non-reflecting boundary conditions for wave propagation problems. First we evaluate a proposed Perfectly Matched Layer (PML) method for the simulation of advective acoustics. It is shown that the proposed PML becomes unstable for a certain combination of parameters. A stabilizing procedure is proposed and implemented. By numerical experiments the performance of the PML for a problem with nonuniform flow is investigated. Further the performance for different types of waves, vorticity and sound waves, are investigated.

The second aspect concerns spurious waves, which are introduced by any discretization procedure. We construct discrete boundary conditions, that are non-reflecting for both physical and spurious waves, when combined with a fourth order accurate explicit discretization of one-way wave equations. The boundary condition is shown to be GKS-stable.

The boundary conditions are extended to hyperbolic systems in two space dimensions, by combining exact continuous non-reflecting boundary conditions and the one dimensional discretely non-reflecting boundary condition. The resulting boundary condition is localized by the standard Padé approximation.

Numerical experiments reveal that the resulting method suffers from *boundary instabilities*. Analysis of a related continuous problem suggests that the discrete boundary condition can be stabilized by adding tangential viscosity at the boundary. For the lowest order Padé approximation we are able to stabilize the discrete boundary condition.

ISBN 91-7283-628-8 • TRITA-NA-0326 • ISSN 0348-2952 • ISRN KTH/NA/R--03/26--SE



# Preface

This thesis consists of an introduction and two papers.

**Paper I:** Daniel Appelö and Gunilla Kreiss, *Evaluation of a Well-posed Perfectly Matched Layer for Computational Acoustics*. In Hyperbolic Problems: Theory, Numerics, Applications, Proceedings of the Ninth International Conference on Hyperbolic Problems (Hyp2002), Pasadena 2002

The author of this thesis contributed to the ideas presented, performed the numerical simulations and wrote the manuscript. The author also presented the paper at Hyp2002.

**Paper II:** Daniel Appelö and Gunilla Kreiss, *Stabilized Local Non-reflecting Boundary Conditions for High Order Methods*. Technical Report, NADA, Royal Institute of Technology, (2003).

Presented by the author at "Waves 2003, Mathematical and Numerical Aspects of Wave Propagation, Jyväskylä, Finland 30 June - 4 July 2003"

Parts of the paper have been published in the proceedings of Waves 2003.

The author contributed to the ideas presented, performed the numerical simulations and wrote the manuscript.



# Acknowledgments

I wish to thank my advisor Prof. Gunilla Kreiss, for all her support, guidance and encouragement throughout this work.

I would also like to thank all my friends and colleagues at NADA. Especially I would like to thank Katarina Gustavsson and O-P Åsén for reading parts of this thesis and making suggestions for improvement.

Financial support from Vetenskapsrådet, Norfa, Generaldirektör Waldemar Borgemans stipendiefond and Erik Petersohns minnesfond is gratefully acknowledged.

Finally I want to extend a big and special thanks to Veronica.



# Chapter 1

## Introduction

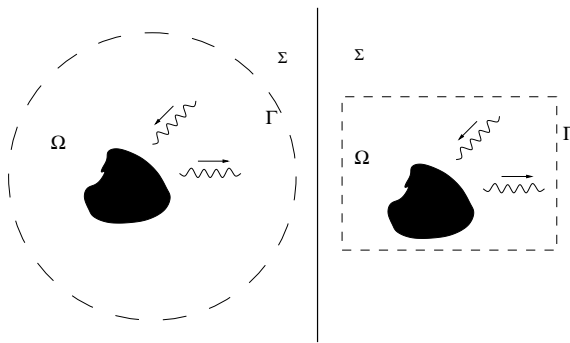


**Figure 1.1.** Two possible truncations  $\Omega$  of an unbounded domain at an artificial boundary  $\Gamma$ . Here  $\Sigma$  is the tail or residual, i.e the union of  $\Sigma$  and  $\Omega$  is the original unbounded domain.

Many interesting problems appearing in physics, biology and other natural sciences have solutions consisting of waves. An important part of these problems are posed on unbounded domains. To compute a numerical solution to such problems, it is necessary to truncate the unbounded domain, due to finite computational resources. This is done by introducing an artificial boundary  $\Gamma$ , see Figure 1.1, defining a new domain  $\Omega$ , which we will refer to as the computational domain. For the problem to be well-posed, it must be closed with a suitable boundary condition on  $\Gamma$ .

To obtain a solution (on  $\Omega$ ) close to the solution on the unbounded domain, the boundary condition on  $\Gamma$  has to be correctly imposed. Usually the artificial boundary  $\Gamma$  is placed in the far field where the solution is composed of waves traveling out of  $\Omega$ . The fundamental observation is therefore that all reflections

caused by the boundary condition on  $\Gamma$  will contaminate the solution in the interior. Hence, an exact boundary condition should prevent all reflections at the boundary as indicated by the name non-reflecting boundary conditions.

The construction of non-reflecting boundary conditions for wave propagation problems has been a matter of ongoing research for over thirty years. The level of difficulty of constructing a particular boundary condition is determined by the underlying problem. It is possible to divide the boundary conditions into four different categories based on the underlying problem. In increasing order of difficulty they are

- Linear time-harmonic wave propagation problems,
- Linear constant coefficient time-dependent wave propagation problems,
- Linear variable coefficient time-dependent wave propagation problems,
- Nonlinear time-dependent wave propagation problems.

To date, there are accurate and efficient boundary conditions available for linear time-harmonic problems (see the review articles [20, 22, 71]) and we do not consider this problem here.

For linear constant coefficient time-dependent wave propagation problems, there are non-reflecting boundary conditions available which work well for some specific problems. An example is the Maxwell equations, where the perfectly matched layer (discussed below) is used today with satisfactory results. On the other hand, for the equations of acoustics, the development of efficient non-reflecting boundary conditions for uniform flows is quite novel.

For the linear variable coefficient time-dependent wave problems and the nonlinear time-dependent wave problems very little has been done and there are many challenging problems left.

In this introduction we consider boundary conditions for linear constant coefficient time-dependent wave problems. Particularly we are interested in boundary conditions which are easy to implementation in a stable and effective fashion, with respect to both memory and time consumption.

A possible categorization of the non-reflecting boundary conditions available is the following: **exact non-reflecting boundary conditions**, **local non-reflecting boundary conditions** and **absorbing boundary layers**.

The remaining part of this introduction will be organized as follows. In chapters 2-4 we give a brief review of exact non-reflecting boundary conditions, local non-reflecting boundary conditions and absorbing boundary layers. In chapter 5 we give a summary of the presented papers.

Throughout this thesis we will limit the discussion to problems governed by the wave equation, Maxwell equations and the linearized Euler equations. By limited modifications many of the methods discussed below can be applied to other equations.

Finally we note that there are a number of review articles available which provide a more complete overview of the subject [16, 22, 37, 38, 71, 72].



## Chapter 2

# Exact Boundary Conditions

A boundary condition can be defined as a procedure

$$B_E u = 0, \quad \text{on } \Gamma.$$

Especially, the boundary condition is said to be exact if the solution  $u$ , of some PDE closed with boundary conditions at infinity, on the unbounded domain is identical to the solution on the bounded domain  $\Omega$  closed by the boundary condition defined by  $B_E$ .

Exact boundary conditions, as will be seen below, will in general be nonlocal both in space and time. The non-locality in time requires the storage of full temporal history of the solution on the boundary if the exact boundary condition is to be used.

In the past, storage requirements have been thought of as an irreparable hindrance for the use of exact non-reflecting boundary conditions in computations. But, as we will see later, there are novel methods available which reduce storage of the history of the solution. Further, these methods make use of fast algorithms which reduce the work per timestep needed to update the exact boundary conditions.

The exact boundary condition  $B_E$  will depend on the shape of  $\Gamma$  and it may be difficult to find an explicit representation of  $B_E$ , if the shape of  $\Gamma$  is too complicated. In the following sections we will present some exact boundary conditions for common choices of  $\Gamma$ .

### 2.1 Planar Boundaries

We start by considering the construction of exact non-reflecting boundary conditions for the two dimensional wave equation in Cartesian coordinates

$$\frac{\partial^2 u}{\partial t^2} = \frac{\partial^2 u}{\partial x^2} + \frac{\partial^2 u}{\partial y^2}, \quad (2.1)$$

solved on the half plane  $x \geq 0$ .

This problem was first considered in the famous paper by Engquist and Majda [18]. They use that any leftgoing solution  $u(x, y, t)$  to (2.1) can be represented by a superpositions of plane waves traveling to the left. Such plane waves are given by

$$u = ae^{i(\sqrt{\xi^2 - \omega^2}x + \xi t + \omega y)}. \quad (2.2)$$

Here  $a$  is the amplitude and  $(\xi, \omega)$  are the duals of  $(t, y)$  satisfying  $\xi^2 - \omega^2 > 0$  and  $\xi > 0$ .

Engquist and Majda conclude that for fixed  $(\xi, \omega)$  the condition

$$\left( \frac{d}{dx} - i\sqrt{\xi^2 - \omega^2} \right) u|_{x=0} = 0$$

annihilate plane waves described by (2.2). For that particular plane wave, this will be an exact non-reflecting boundary condition. For a more general wave packet, the exact non-reflecting boundary condition is obtained by superposition of boundary conditions for the plane waves, described above. For waves supported by the wave equation, (2.1) the exact non-reflecting boundary condition becomes

$$\mathcal{F} \left( \frac{\partial u}{\partial x} \right) - i\sqrt{\xi^2 - \omega^2} \mathcal{F}u = 0, \quad \text{on } x = 0, \quad (2.3)$$

where  $\mathcal{F}v(x, \omega, \xi) = \int_{-\infty}^{\infty} \int_{-\infty}^{\infty} e^{-i(\xi t + \omega y)} v(x, y, t) dy dt.$

The non-locality of the above boundary condition is clearly manifested through the integral transforms. Inverting the transforms directly is not possible since the function  $\sqrt{\xi^2 - \omega^2}$  does not have an explicit inverse transform. To represent (2.3) in the physical domain, Engquist and Majda use the pseudo-differential operator which has the symbol  $\sqrt{\xi^2 - \omega^2}$ .

Another useful tool which has been used to derive exact boundary conditions is the Dirichlet to Neumann (DtN) map. The DtN map is an operator relating the Dirichlet datum to the Neumann datum on the boundary  $\Gamma$ . This is done to enforce the desired asymptotic behavior of the solution at infinity. A more formal definition of the DtN map can be found in e.g. Ramm [60]. Here we restrict ourselves to motivating its use by the following example used to derive an alternative formulation of (2.3).

Consider solutions to the Helmholtz equation posed on the residual domain  $\Sigma$

$$s^2 \hat{u} = \nabla^2 \hat{u}, \quad x \in \Sigma, \quad (2.4)$$

with boundary conditions at infinity identical to those used for  $\Xi \equiv \Sigma \cup \Omega$ . Since no boundary condition have been imposed on  $\Gamma$ , there are infinitely many solutions satisfying the above equation. However, the solution on  $\Xi$  must be one of these.

The desired solution  $\hat{u}$  coinciding with the solution on  $\Xi$  can be singled out by a specific choice of the operator  $\mathcal{D}$

$$\frac{\partial \hat{u}}{\partial n} = -\hat{\mathcal{D}}\hat{u}, \quad x \in \Gamma.$$

$\mathcal{D}$  defines the DtN map. Here the normal is taken outward from  $\Omega$ . The DtN map can be used to define the exact boundary condition  $B_E$

$$B_E u \equiv \frac{\partial u}{\partial n} + \mathcal{L}^{-1} \left( \hat{\mathcal{D}} \mathcal{L} u \right), \quad (2.5)$$

where  $\mathcal{L}$  denotes the Laplace transform.

Now, (2.5) can be used to derive the exact boundary condition for (2.1) at a planar boundary. As before we assume that (2.1) is solved for  $\Omega$  being the half plane  $x > 0$ . Hence to derive the DtN map we consider solutions which are bounded on  $\Sigma$ . By taking the Fourier and Laplace transform (with the duals  $(k, s)$ ) of (2.1) we obtain the ordinary differential equation

$$\frac{\partial^2 \tilde{u}}{\partial x^2} = (s^2 + |k|^2) \tilde{u}, \quad x \in \Sigma.$$

For  $\Re s > 0$ , solutions that are bounded on  $\Sigma$  can be written as

$$a e^{\sqrt{s^2 + |k|^2} x},$$

and the DtN map is therefore defined by

$$\tilde{\mathcal{D}} = -\sqrt{s^2 + |k|^2}.$$

Here the the branch of the square root is chosen so that  $\tilde{\mathcal{D}}$  is analytical and positive for  $\Re s > 0$ . By inserting  $\tilde{\mathcal{D}}$  into (2.5) we see that the exact boundary condition is identical to the boundary condition (2.3) for  $t > 0$ .

In [35], Hagstrom derives a formulation of (2.3) which only includes the inverse Fourier transform in the y direction and a convolution in time. By rewriting  $\tilde{\mathcal{D}}$  as

$$\tilde{\mathcal{D}} = -s - (\sqrt{s^2 + |k|^2} - s),$$

and using that  $\hat{K}(s) = \sqrt{s^2 + |k|^2} - s$  for the function

$$K(t) \equiv \frac{J_1(t)}{t} = \frac{1}{\pi} \int_{-1}^1 \sqrt{1 - \rho^2} \cos \rho t \, d\rho,$$

Hagstrom obtains the formulation

$$\frac{\partial u}{\partial n} - \frac{\partial u}{\partial t} - \mathcal{F}^{-1} (|k|^2 K(|k|t) * \mathcal{F} u) = 0. \quad (2.6)$$

By the use of fast algorithms for the computation of convolutions, see [41], together with the fast Fourier transform, (2.6) may be directly imposed. The number

of operations required to evaluate the boundary condition would then be acceptable. However the fact that the solution on the boundary has to be stored at all time levels makes the storage requirements unacceptable for late times. Fortunately, as we will see later, there is a cure to this.

Note that there is no explicit need for a two dimensional setting in the above examples. The analysis is identical if  $\Gamma$  is chosen as the hyper plane  $x = 0$ . The Fourier transform is then to be interpreted as the multidimensional Fourier transform.

## 2.2 Spherical Boundary

Consider the homogeneous wave equation posed on the tail  $\Sigma$  in three dimensions. If the boundary  $\Gamma$  has the shape of a sphere of radius  $R$ , we can express the solutions to Helmholtz equation

$$\hat{s}^2 \hat{u} = \nabla^2 \hat{u}, \quad x \in \Sigma,$$

in spherical harmonics

$$\hat{u} = \sum_{l=0}^{\infty} \sum_{m=-l}^l \bar{u}_{lm}(r) Y_l^m(\theta, \phi).$$

The functions  $\bar{u}_{lm}$  satisfy the equation

$$\frac{\partial^2 \bar{u}_{lm}}{\partial r^2} + \frac{2}{r} \frac{\partial \bar{u}_{lm}}{\partial r} - \left( s^2 + \frac{l(l+1)}{r^2} \right) \bar{u}_{lm} = 0. \quad (2.7)$$

As before, we require the solution to be bounded at infinity which leads to the solution of (2.7)

$$\begin{aligned} \bar{u}_{lm}(r, s) &= \frac{k_l(rs)}{k_l(Rs)} \bar{u}_{lm}(R, s), \\ k_l(z) &= \frac{\pi}{2z} e^{-z} \sum_{k=0}^l \frac{(l+k)!}{k!(l-k)!} (2z)^{-k}. \end{aligned}$$

The DtN map is obtained by taking the logarithmic derivative of  $k_l$

$$\frac{sk'_l(Rs)}{k_l(Rs)} = -s - \frac{1}{R} - \frac{1}{R} \hat{S}_l, \quad \hat{S}_l = \frac{\sum_{k=0}^{l-1} \frac{(2l-k)!}{k!(l-k-1)!} (2Rs)^k}{\sum_{k=0}^l \frac{(2l-k)!}{k!(l-k)!} (2Rs)^k}. \quad (2.8)$$

By summation over all harmonics, inverse Laplace transform we obtain the exact non-reflecting boundary condition

$$\frac{\partial u}{\partial r} + \frac{\partial u}{\partial t} \frac{1}{R} u + \frac{1}{R^2} \mathcal{H}^{-1}(S_l * (\mathcal{H}u)_l) = 0, \quad r = R, \quad (2.9)$$

where  $\mathcal{H}$  denote the spherical harmonic transform. The function  $S_l$  is defined through its Laplace transform  $\hat{S}_l$  found in (2.8).

A fundamental property of the function  $S_l$  is that since its Laplace transform  $\hat{S}_l$  is a rational function of degree  $(l-1, l)$  it can be represented as a sum of  $l$  exponential functions in the temporal domain. Using the fact that a convolution between an exponential function and a function  $v(t)$

$$\eta(t) = \int_0^t \alpha e^{-\beta(t-\tau)} v(\tau) d\tau,$$

can be rewritten as

$$\frac{d\eta}{dt} + \beta\eta = \alpha v, \quad v(0) = 0,$$

it is possible to localize the exact boundary condition (2.9). This was independently discovered by Sofronov [63, 64] and Grote and Keller [30, 31]. In [31] the boundary conditions (2.9) are used with both finite difference and finite element approximations of the three dimensional wave equation. Numerical simulations are presented and uniqueness and stability is discussed. Grote and Keller have also successfully adopted the methods used in [30, 31] to other scattering problems [28, 29, 32, 33].

Since the spherical harmonics decomposition is formulated as an infinite series it is necessary to truncate the series at some  $l \leq L_0$ . The obvious way to truncate by retaining the first  $L_0$  harmonics will lead to extensive memory requirements, if  $L_0$  is large. This is due to the fact that the number of auxiliary variables which must be introduced are proportional to  $L_0$ . Especially this is true if the solution has a high harmonic content which means that  $L_0$  has to be chosen large.

Norm minimizing rational approximants for convolution kernels are introduced by Alpert et al. in [5, 6]. They make it possible to distribute the error equally over all harmonics. Alpert et al. study the problem of approximating a convolution kernel  $\kappa(t)$ , as  $\mathcal{S}_l$  or  $\mathcal{K}$ , by approximating its Laplace transform  $\hat{\kappa}(s)$  by a function  $\hat{\mathcal{K}}(s)$  represented as a sum of poles

$$\hat{\mathcal{K}}(s) = \sum_{l=1}^L \frac{p_l}{s + s_l}.$$

Inverse Laplace transform of  $\hat{\mathcal{K}}(s)$ . If we require  $\Re s_l > 0$ , gives

$$\mathcal{K}(t) = \sum_{l=1}^L p_l e^{-s_l t}.$$

As has been noted above, convolution with the kernel  $\mathcal{K}(t)$  can be reduced to advancing  $L$  ordinary differential equations with homogeneous initial data.

The motivation of the approximation of the Laplace transformed kernel is found by using Parseval's relation on the two convolutions  $f = K * g$  and  $\psi = \kappa * g$

$$\|f - \psi\|_2 = \|\hat{\mathcal{K}}\hat{g} - \hat{\kappa}\hat{g}\|_2 \leq \left\| \frac{\hat{\mathcal{K}} - \hat{\kappa}}{\hat{\mathcal{K}}} \right\|_\infty \|\mathcal{K} * g\|_2.$$

Assuming that the kernel  $\kappa$  is approximated with an error in norm  $\epsilon$  for  $m$  harmonics, Alpert et al. are able to prove that this can be done by a fixed small number of poles  $L \ll m$ . Moreover, for the kernels appearing for a spherical and cylindrical boundary, the error bound holds for *all times*. For example in [5] it is shown that for 1024 harmonics it is sufficient to use 21 poles for approximating  $\mathcal{S}_l$  with an error  $\epsilon \leq 10^{-8}$ . This can be compared to the direct truncation which would require all 1024 harmonics if the solution have high harmonic content close to the boundary. The number of needed auxiliary variables can clearly be reduced by the approximation technique suggested by Alpert et al.

For the approximation of the kernel used at a planar boundary the error bound has a weak dependence on time. But for the 1024 harmonics example discussed above,  $\epsilon \leq 10^{-8}$  holds for times  $t < 10000$ .

Although (2.9) can be localized in time, it is still nonlocal in space. Therefore, to reduce the operation count it is important to use some fast procedure for the direct and inverse harmonic transforms. The derivations of such transforms are quite novel and may be found in e.g. Mohlenkamp[57], Suda and Takami [65] and Healy et al. [42].

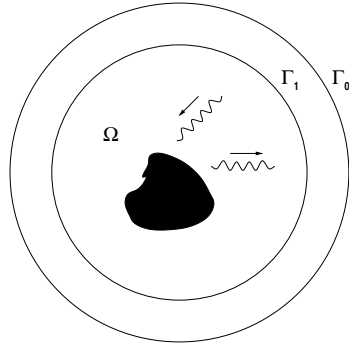


**Figure 2.1.** The non-reflecting boundary conditions based on retarded potentials suggested by Ting and Miksis requires two artificial boundaries.

Before considering the construction of exact non-reflecting boundary conditions for first order hyperbolic systems, we briefly discuss two additional exact boundary conditions for the wave equation in three dimensions. The first boundary condition is based on the exact representation of the solution by retarded potentials. It was originally devised by Ting and Miksis [69] and later implemented by Givoli and Cohen [24].

The boundary condition requires two artificial boundaries  $\Gamma_0$  and  $\Gamma_1$  as in Figure 2.1. The solution on  $\Gamma_0$  can be represented by the retarded potential formula

$$u(x, y) = -\frac{1}{4\pi} \int_{\Gamma_1} \left( u(y, t-r) \frac{\partial}{\partial n} \frac{1}{r} - \frac{1}{r} \frac{\partial u(y, t-r)}{\partial n} - \frac{1}{r} \frac{\partial r}{\partial n} \frac{\partial u(y, t-r)}{\partial t} \right) dy, \quad (2.10)$$

$$r = |x - y|, \quad x \in \Gamma_0.$$

The above formula is nonlocal in time but the temporal history of the solution needed to be stored is bounded by the maximum travel time between points on the boundary. The cost of a direct evaluation of the integral is proportional to the square of the points used to discretize the boundary. Again this can be sped-up by fast methods, see [19]. Finally, it should be noted that in the implementation presented in [24] there was a need for artificial damping to keep the method stable.

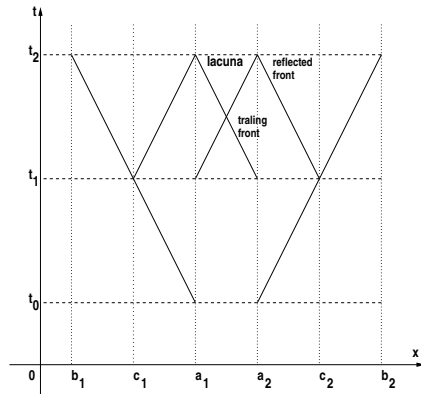


**Figure 2.2.** Sketch of waves generated by a source with finite support illustrating the existence of lacuna.

A direct consequence of the formula (2.10) is the strong Huygens' principle or the existence of lacunae. The phenomena lacunae can be illustrated by considering the wave equation in one dimension with a forcing compactly supported in space and time and homogeneous initial data, i.e.

$$\frac{\partial^2 u}{\partial t^2} - c^2 \frac{\partial^2 u}{\partial x^2} = f, \quad (2.11)$$

$$\frac{\partial u(x, 0)}{\partial t} = 0, \quad u(x, 0) = 0, \quad (2.12)$$

$$\text{supp } f = \{(x, t) \mid x \in [a_1, a_2], t_0 < t < t_1\}. \quad (2.13)$$

At time  $t = t_0$  waves will start to be generated on the domain  $[a_1, a_2]$  as shown in Figure 2.2. At a later time  $t_2$ , they can at most have traveled to the points  $b_1$  and

$b_2$ , determined by the wave speed  $c$ . Now since waves are only generated between times  $t_0 < t < t_1$ , there will be no waves inside the domain  $[a_1, a_2]$  at times  $t > t_2$ . The domain  $[a_1, a_2]$  is now inside the lacuna. If we are to construct non-reflecting boundary conditions at  $a_1$  and  $a_2$  we know that at times  $t > t_2$  and  $t < t_0$  the exact boundary condition is a homogeneous Dirichlet condition (the existence of lacuna). At the times in between we may compute the solution on a slightly larger domain  $[c_1, c_2]$  with e.g. periodic boundary conditions. The domain  $[c_1, c_2]$  is chosen so that waves reflected at the boundary does not influence the solution in  $[a_1, a_2]$  for times  $t_0 < t < t_2$ .

The existence of lacunae have been used by Ryabenkii, Tsynkov and Turchaninov [62] to construct exact non-reflecting boundary conditions for the wave equation in odd dimensions by partitioning the source term in time. Note that the existence of lacunae is restricted to odd space dimensions.

### 2.3 First Order Hyperbolic Systems

Here we consider construction of exact non-reflecting boundary conditions for a first order, constant coefficient, strongly hyperbolic system. The boundary conditions are imposed at a planar boundary,  $x = 0$ . In the domain  $\Omega$ , ( $x > 0$ ) the system can be written as

$$\frac{\partial u}{\partial t} + A \frac{\partial u}{\partial x} + \sum_j B_j \frac{\partial u}{\partial y_j} = 0, \quad (2.14)$$

where  $u \in \mathbb{R}^n$ ,  $A, B_j \in \mathbb{R}^{n \times n}$ . If we further assume that  $A$  is invertible (no characteristic boundary conditions) we can employ the usual Fourier and Laplace transform to obtain

$$\frac{\partial \tilde{u}}{\partial x} = M \tilde{u}, \quad M = -A^{-1} \left( sI + \sum_j ik_j B_j \right). \quad (2.15)$$

Since we consider a strongly hyperbolic problem, we can decompose the solution into left and right-going modes or waves. The right-going waves are those corresponding to positive eigenvalues of  $M$  and the left-going, those who correspond to negative eigenvalues.

The decomposition

$$QMQ^{-1} = \begin{bmatrix} \lambda_R & 0 \\ 0 & \lambda_L \end{bmatrix} \equiv \Lambda,$$

where  $Q$  is composed of the the eigenvectors of  $M$  arranged in two matrices  $Q_R, Q_L$  such that

$$Q = \begin{bmatrix} Q_R \\ Q_L \end{bmatrix},$$

can be used to decouple the system into two sets of scalar equations

$$\frac{\partial \tilde{v}_L}{\partial x} = \lambda_L \tilde{v}_L, \quad \frac{\partial \tilde{v}_R}{\partial x} = \lambda_R \tilde{v}_R, \quad (2.16)$$

where  $\tilde{v} \equiv Q \hat{u}$ . An exact non-reflecting boundary condition which make sure that no waves enter  $\Omega$  at  $x = 0$  is

$$\tilde{v}_R \equiv B_R \hat{u} = 0. \quad (2.17)$$

Note that  $B_R$  can be chosen in many ways. The only restriction of  $B_R$  is that it should be orthogonal to the matrix  $Q_L$ . Therefore a natural choice is  $B_R \equiv Q_R$ . However this choice may not always be suitable. In fact, it can lead to an ill-posed problem. This is the case for the linearized Euler equations and was discovered by Giles in [21], where an alternative choice of  $B_R$ , which leads to a well-posed problem, was suggested. Other choices of  $B_R$  for the linearized Euler equations, leading to a well-posed problem have been suggested by Hagstrom and Goodrich [26, 27] and Colonius and Rowley [61].



## Chapter 3

# Local Non-reflecting Boundary Conditions

In this chapter we begin by presenting some classic local non-reflecting boundary conditions suggested in the literature. Many of these are formulated as hierarchies of conditions of increasing accuracy. Often increasing accuracy is synonymous with introduction of high-order (mixed) derivatives on the boundary. Stable discretization of such derivatives is not trivial. Therefore, in practice, the hierarchical structure have not been exploited properly.

However, boundary conditions containing high-order derivatives can be converted into sequences of conditions containing only low order derivatives. Such boundary conditions are based on the introduction of auxiliary variables and are often referred to as *high-order non-reflecting boundary conditions*. Boundary conditions of that type will be discussed in the later half of this chapter.

In the previous chapter we discussed the exact boundary condition for the two dimensional wave equation at a planar boundary derived by Engquist and Majda. In [18], Engquist and Majda also present a method to localize the exact boundary condition. They conclude that if the function

$$\sqrt{1 - \frac{\omega^2}{\xi^2}}$$

is approximated by some rational function, it is possible to localize the approximation by explicitly inverting the Fourier transforms.

The most natural approximation is perhaps to use a Taylor series expansion, however the resulting local boundary condition leads to an ill-posed problem, and can therefore not be used.

Engquist and Majda investigate the boundary conditions obtained if a Padé expansion is used. The resulting boundary conditions are proved to yield a well-posed problem independent of the order of the expansion. The boundary conditions obtained from the two first Padé expansions are

$$\begin{aligned} B_1 u &\equiv \left( \frac{\partial}{\partial x} - \frac{1}{c} \frac{\partial}{\partial t} \right) u = 0, \\ B_2 u &\equiv \left( \frac{1}{c} \frac{\partial^2}{\partial t \partial x} - \frac{1}{c^2} \frac{\partial^2}{\partial t^2} + \frac{1}{2} \frac{\partial^2}{\partial y^2} \right) u = 0. \end{aligned}$$

Note that in the boundary conditions above, mixed derivatives in time and space appear already in the second order approximation, precluding difficulties of discretization of high-order approximations. The above equations are often referred to as one-way equations in the literature.

The Padé expansion is not the only possible approximation, in fact not even the best (rather the worst at glancing incidence). Other possible expansions (Chebyshev, least-squares, etc) are studied by Trefethen and Halpern in [40, 70], where they also formulate theorems for determining the well-posedness for these types of expansions.

Although [18] is the most well known paper that use one-way equations as non-reflecting boundary condition, it should be noted that it was used in an earlier work by Lindeman [54].

The use of one-way equations as boundary condition has also been studied by Higdon [44]. He constructed an asymptotically ( $m \rightarrow \infty$ ) exact non-reflecting boundary condition by factorization of one-way equations. The non-reflecting boundary condition he proposes is given by

$$B_m u = \left( \prod_{j=1}^m \left( (\cos \alpha_j) \frac{\partial}{\partial x} - c \frac{\partial}{\partial t} \right) \right) u = 0. \quad (3.1)$$

The boundary condition suggested by Higdon is exact for plane waves hitting the boundary at angles  $\pm \alpha_j$ . In the original implementation by Higdon, only boundary conditions with small  $m$  were used.

Bayliss and Turkel [9] work with sequences of local non-reflecting boundary conditions for the wave equation in spherical and cylindrical coordinates. The boundary condition is similar in structure to (3.1) and is given by

$$B_m u = \left( \prod_{j=1}^m \left( \frac{\partial}{\partial t} + \frac{\partial}{\partial r} + \frac{2l-1}{R} \right) \right) u = 0. \quad (3.2)$$

Although the suggested boundary condition is extendible to high-order, only the second order formulation is implemented in [9].

Adoption of the above described classic boundary conditions can be found in many areas of science where wave propagation is present (see e.g. the review articles [22, 71]). However, for these boundary conditions, the hierarchical structure is rarely exploited. Typically only the lowest order terms in the expansions are used in the construction. Adoption of the first order Engquist Majda condition to a first order hyperbolic system yields the so called characteristic boundary conditions. Independent of application, the solution obtained when a low-order boundary condition is used will suffer from  $\mathcal{O}(1)$  error after moderate times.

### 3.1 High-Order Local Non-reflecting Boundary Conditions

Modern high-order local non-reflecting boundary conditions are based on the introduction of auxiliary variables. This technique was first used by Collino [13]. There he considers the following approximation to the exact boundary condition (2.3)

$$\mathcal{F}\left(\frac{\partial u}{\partial x}\right) + i\xi\left(1 - \sum_{m=1}^L \beta_m \frac{\omega^2}{\xi^2 - \alpha_m \omega^2}\right) \mathcal{F}u = 0, \quad x = 0, \quad (3.3)$$

where the coefficients  $\alpha_m, \beta_m$  depend on the type of approximation used,  $L$  is the order of the boundary condition. With

$$\alpha_m = \cos^2\left(\frac{m\pi}{2L+1}\right), \quad \beta_m = \frac{2}{2L+1} \sin^2\left(\frac{m\pi}{2L+1}\right),$$

the Padé expansion used in [18] is recovered.

Collino shows that the boundary condition (3.3) can be reformulated as a sequence of auxiliary problems containing only low order derivatives

$$\begin{aligned} \frac{\partial u}{\partial x} + \frac{\partial u}{\partial t} - \sum_{m=1}^L \beta_m \frac{\partial \psi_m}{\partial t} &= 0, \\ \frac{\partial^2 u}{\partial t^2} - \frac{\partial}{\partial y^2} (\alpha_m \psi_m + u) &= 0, \quad m = 1, \dots, L. \end{aligned}$$

Here  $\psi_m$  are the auxiliary variables introduced on the boundary.

In [13] Collino presents numerical experiments using boundary conditions of different order ( $L \leq 10$ ). The results show that the accuracy of the boundary condition increase monotonically. Long time behavior of the boundary condition is not examined.

The wave equation posed in a semi infinite wave-guide with a planar boundary at  $x = 0$  have been considered by Givoli and Neta in [25]. Inspired by the work of

Hagstrom and Harihan (discussed below) they use the Higdon boundary condition (3.1) to formulate a sequence of auxiliary problems

$$\begin{aligned} \left( \frac{\partial}{\partial x} + \frac{1}{C_m} \frac{\partial}{\partial t} \right) \psi_{m-1} &= \psi_m, \quad m = 1, \dots, L \\ \psi_0 &\equiv u, \quad \psi_L \equiv 0, \end{aligned} \quad (3.4)$$

which converges to the exact boundary condition (2.3) when  $L \rightarrow \infty$ . Since (3.4) contains normal derivatives of  $\psi_m$ , when discretized, they would need to be stored not only on the boundary but also in the interior. This would be unnecessary memory consuming and therefore (3.4) is reformulated to contain only tangential derivatives of second order instead of normal derivatives. In [25] the modified boundary conditions are integrated into an explicit finite difference method which is shown by numerical examples to be stable. Givoli and Neta also give a detailed description of how the coefficients  $C_m$  can be chosen automatically for good performance. It is shown by numerical experiments that accuracy of the method is increasing with  $L$ . This holds for late times.

Hagstrom and Harihan constructed the first reformulation of (3.2) using auxiliary variables. It was presented in [36, 39] where they consider the wave equation in both spherical and cylindrical coordinates. They also extend the boundary condition to the two dimensional Maxwell equations in cylindrical coordinates.

The recursion formula proposed in [39] requires the introduction of  $L$  auxiliary variables and is given by

$$\begin{aligned} \left( \frac{\partial}{\partial t} + \frac{m}{R} \right) \psi_{m-1} &= \frac{1}{2R^2} (\nabla_R^2 + m(m-2)) \psi_m + \frac{1}{2} \psi_m, \quad m = 1, \dots, L, \\ \psi_0 &= u, \quad \psi_L = 0, \end{aligned}$$

where  $\nabla_R^2$  is the Laplace operator on a sphere with radius  $R$ . The boundary conditions are implemented using finite differences and results, showing a rapid decay of the error as  $L$  increase, are presented.

In [23], Givoli constructed high-order non-reflecting boundary conditions for the time-dependent and time-harmonic wave equation in two dimensions in cylindrical coordinates. Givoli uses that local non-reflecting boundary conditions can be written on the form

$$-\frac{\partial u}{\partial r} = L_K u, \quad \text{on } \Gamma,$$

where  $L_K$  is a differential operator of order  $K$ .

By considering the time-harmonic wave equation, Givoli is able to construct high-order boundary condition which lead to a symmetric finite element discretization. The method is also extended to the time-dependent case with the symmetric properties unaltered. Due to symmetry, the resulting finite element discretization is stable and well-conditioned for all  $K$ .

As we have seen above the operator  $L_K$  can be formulated with normal or tangential derivatives or a mix of both. Givoli derives a boundary condition for an operator containing only tangential derivatives of even order. To make the boundary condition more general, Givoli also give algorithms which translate different formulations of  $L_K$  into a form which fit into the high-order boundary condition he proposed. In [23] only results for the time-harmonic wave equation is presented.

We close this section by noting that the high-order non-reflecting boundary conditions considered here have been constructed in the context of the wave equation. Due to the the novelty of these methods, extensions to other problems are limited but this will surely change with time.



## Chapter 4

# Absorbing Boundary Layers

An alternative to exact or high-order local non-reflecting boundary conditions is to surround the computational domain with a finite width, absorbing layer. Typical setups are pictured in Figure 4.1. Ideally, all waves traveling into the layer, independent of frequency or angle of incidence, should be absorbed to such extent that reflections at the outermost boundary are of no importance. Absorbing layers

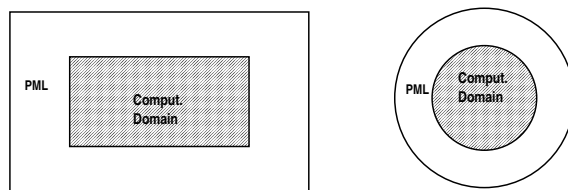


**Figure 4.1.** The computational domain is surrounded by an absorbing layer (PML). Different geometries are possible.

with this ideal properties do exist, and are referred to as Perfectly Matched Layers (PML). They were first introduced in the context of computational electromagnetics, where they are considered as state of the art and are widely used in practical computations. Also in computational acoustics the PML technique has had an impact. However its performance seems to be not quite as good as for computational electromagnetics.

## 4.1 Absorbing Boundary Layers for Computational Electromagnetics

The idea of surrounding the computational domain with an absorbing layer was studied by Israeli and Orzag [49] and Kosloff and Kosloff [51]. The proposed absorbing layers only worked well for waves of normal incidence and they were not commonly used in computations. Karni [50] devised an absorbing layer that is reflectionless for waves propagating in a given direction but still causes too much reflections for other waves.

The major breakthrough, which made absorbing boundary conditions competitive, was the introduction of the Perfectly Matched Layer by Berenger [12]. Berenger considers the form of Maxwell equations describing transverse electrical (T-E) waves in two dimensions

$$\begin{aligned}\varepsilon_0 \frac{\partial E_x}{\partial t} + \sigma E_x &= \frac{\partial H_z}{\partial y}, \\ \varepsilon_0 \frac{\partial E_y}{\partial t} + \sigma E_y &= -\frac{\partial H_z}{\partial x}, \\ \mu_0 \frac{\partial H_z}{\partial t} + \sigma^* H_z &= \frac{\partial E_x}{\partial y} - \frac{\partial E_y}{\partial x}.\end{aligned}\tag{4.1}$$

Here  $E_x$  and  $E_y$  are the electric fields,  $H_z$  the magnetic field,  $\varepsilon_0$  and  $\mu_0$  are the free space permittivity and permeability and  $\sigma$  and  $\sigma^*$  the electric and magnetic conductivity. By the simple, but unphysical, splitting  $H_z = H_{zx} + H_{zy}$ , Berenger introduced the Perfectly Matched Layer as a medium governed by the equations

$$\begin{aligned}\varepsilon_0 \frac{\partial E_x}{\partial t} + \sigma_x E_x &= \frac{\partial(H_{zx} + H_{zy})}{\partial y}, \\ \varepsilon_0 \frac{\partial E_y}{\partial t} + \sigma_y E_y &= -\frac{\partial(H_{zx} + H_{zy})}{\partial x}, \\ \mu_0 \frac{\partial H_{zx}}{\partial t} + \sigma_x^* H_{zx} &= -\frac{\partial E_y}{\partial x}, \\ \mu_0 \frac{\partial H_{zy}}{\partial t} + \sigma_y^* H_{zy} &= \frac{\partial E_x}{\partial y}.\end{aligned}\tag{4.2}$$

For the particular choice  $\sigma_x = \sigma_y = \sigma_x^* = \sigma_y^* = 0$  (4.2) is reduced to Maxwell equations for vacuum.

In [12], Berenger shows that media described by  $(\sigma_x, \sigma_x^*, 0, 0)$  or  $(0, 0, \sigma_y, \sigma_y^*)$ , where  $\sigma$  and  $\sigma^*$  satisfy  $\sigma^* \varepsilon_0 = \sigma \mu_0$ , does not produce any reflections at a vacuum-medium interface normal to  $x$  and  $y$  respectively. Furthermore, waves traveling across the interface decay exponentially inside the media at a rate depending on the magnitude of the conductivity parameters  $\sigma$  and  $\sigma^*$ .

The equations (4.2) suggest that the conductivity parameters  $\sigma$  and  $\sigma^*$  should be chosen constant and large for the solution to decay rapidly in the PML. However,

if a constant  $\sigma$  and  $\sigma^*$  is used in numerical computations there will be reflections at the interface due to the discontinuity of  $\sigma$  at the vacuum-medium interface. Instead the conductivity parameters are typically chosen as a function vanishing at the interface and increasing monotonically to some moderate value at the outermost boundary.

The possibility to tune the conductivity parameters  $\sigma$  and  $\sigma^*$  is an advantage of the method, but it can also be an inconvenience if it should be chosen automatically. To our knowledge there is no known algorithm for an optimal choice of the conductivity parameters for a general numerical method although the choice is critical for the performance of a PML.

Optimal choices of the conductivity parameters have been investigated for specific discretizations by Collino and Monk [15] and Asvadurov et al. [8]. The latter presents an idea based on optimization of the grid inside the PML rather than the conductivity parameters.

When Berenger introduced his PML the efficiency of it was far better than previously known boundary conditions [66]. Moreover, it was straightforward to implement and incorporate into existing codes due to its similarity in structure to the Maxwell equations. These features lead to that the PML-technique was adopted in many other areas of research. For example Collino constructed PML equations for the paraxial equations [14], and for the linearized Euler equations Hu [45] and Tam et al. [67] have derived split-field PML equations.

#### 4.1.1 Well-Posed Perfectly Matched Layer

In this section we will discuss the well-posedness (see e.g. [52]) of different PML. Therefore we first introduce the definition of well-posedness for a Cauchy problem.

**Definition** *The Cauchy problem is well-posed if the following two conditions are satisfied*

- (I) *There exist constants  $K > 0$  and  $\alpha \in \mathbb{R}$  such that for all  $U(\cdot, 0) \in L_2$  there exists a unique solution  $U(\cdot, t) \in L_2$  that satisfies*

$$\|U(\cdot, t)\|_{L_2} \leq Ke^{\alpha t} \|U(\cdot, 0)\|_{L_2}, \quad (4.3)$$

- (II) *Any zero order perturbation of the Cauchy problem satisfies (I).*

We will also use the concept of a weakly well-posed problem, meaning a problem satisfying condition (I) but not (II). By this definition a strongly hyperbolic problem is well-posed but a weakly hyperbolic problem can only be weakly well-posed.

Unfortunately the split-field PML introduced by Berenger was shown by Abarbanel and Gottlieb [1] to be only weakly well-posed. It was believed that the split-field PML (4.2) could become ill-posed under zero order perturbations. An example of such a perturbation for the PML equations was presented in [1].

Although being only weakly well-posed, the PML of Berenger has been used in practical computations with success (see e.g. [66]). It also seems that for computations with moderately refined grids, and not too long simulation times, it behaves well. Recently, Bécache and Joly [10] showed by energy estimates that Berengers PML has at worst linearly growing solutions at late times.

There are however several PML formulations for Maxwell equations which are well-posed. An example is the PML derived by Ziolkowski [74]. Ziolkowski used a Lorenz material model, which is based on physical considerations, to derive an un-split PML. Zhao and Cangellaris use similar ideas in [73], and their PML is often referred to as the standard un-split PML, in the literature. In [59], Petropoulos derives PML formulations, based on the standard un-split PML, for rectangular, cylindrical and spherical coordinates.

Another PML formulation obtained from mathematical reasoning is proposed by Abarbanel and Gottlieb [2]. They assume that the behavior of the absorbing layer can be described by lossy Maxwell equations. For a T-E case they start with

$$\begin{aligned}\frac{\partial E_x}{\partial t} &= \frac{\partial H_z}{\partial y} + R_1, \\ \frac{\partial E_y}{\partial t} &= -\frac{\partial H_z}{\partial x} + R_2, \\ \frac{\partial H_z}{\partial t} &= \frac{\partial E_x}{\partial y} - \frac{\partial E_y}{\partial x} + R_3,\end{aligned}\tag{4.4}$$

and look for solutions satisfying

$$\begin{pmatrix} H_z \\ E_x \\ E_y \end{pmatrix} = \begin{pmatrix} 1 \\ \Omega_1(x; \alpha, \beta, \omega) \\ \Omega_2(x; \alpha, \beta, \omega) \end{pmatrix} e^{i\omega(t-\alpha x-\beta y)} e^{-\alpha \int_0^x \sigma(\eta) d\eta}$$

The unknown functions  $R_1, R_2, R_3, \Omega_1, \Omega_2$  are determined by the constraints that

- $R_i$ , ( $i = 1, 2, 3$ ) should be independent of the parameters  $\alpha, \beta, \omega$ ,
- the solution should be continuous across the interface,
- the amplitude of the solution vector in the layer should be monotonically decreasing.

In the derivation they use the dispersion relation

$$\alpha^2 + \beta^2 = 1,\tag{4.5}$$

to eliminate the  $\beta$  dependence in  $\Omega_1, \Omega_2$ . These constraints, which makes sure that the absorbing layer is perfectly matched, yield a set of PML equations

$$\begin{aligned}\frac{\partial E_x}{\partial t} &= \frac{\partial H_z}{\partial y}, \\ \frac{\partial E_y}{\partial t} &= -\frac{\partial H_z}{\partial x} - 2\sigma E_y - \sigma P, \\ \frac{\partial H_z}{\partial t} &= \frac{\partial E_x}{\partial y} - \frac{\partial E_y}{\partial x} + \sigma' Q, \\ \frac{\partial P}{\partial t} &= \sigma E_y, \\ \frac{\partial Q}{\partial t} &= -\sigma Q - E_y.\end{aligned}\tag{4.6}$$

Note that the question of well-posedness is trivial since the equation (4.6) is only a zero order perturbation of (4.1) which is well posed. The auxiliary variables  $P, Q$  only appear as ordinary differential equations and will not alter the well-posedness.

### 4.1.2 Long Time Behavior of Well-posed PML

The requirement of well-posedness of a PML is crucial for its use in numerical computations. However, well-posedness allows exponential growth, hence there may be modes growing in time in a well-posed PML. This is not desired. The natural demand that a PML should be absorbing has been incorporated in the definition of a stable well-posed PML introduced by Bécache and Joly [10]. The definition of a stable well-posed PML is closely related to the above definition of well-posedness.

**Definition** *A system which is a zero order perturbation of a first order hyperbolic system is (weakly) stable if it is (weakly) well-posed and (4.3) holds with  $\alpha \leq 0$ .*

In [4] Abarbanel, Gottlieb and Hesthaven studied the long time behavior of two well-posed PML [2], [74] for computational electromagnetics. They show by computations and analytical argumentation that both PML methods are unstable in the sense discussed above. They suggest a remedy to these instabilities which alter the perfect matching only slightly. By computations they demonstrate that the stabilized PML can perform equally well.

Another remedy to the problem of late time instabilities in the un-split PML for Maxwell equations in two dimensions was found by Bécache, Petropoulos and Gedney [11]. They propose an un-split PML based on [59] for which they are able to prove energy estimates for the solution inside the PML. The energy estimates guarantee that there is no growth in the energy of the solution. Moreover, the suggested PML is truly perfectly matched at the vacuum/PML interface in contrary to the stabilized PML described in [4].

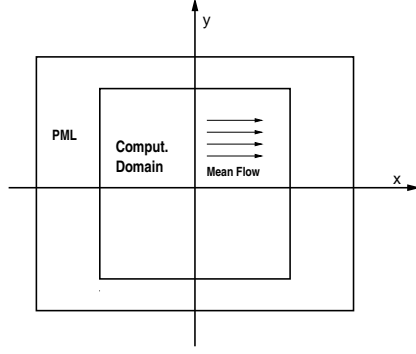


**Figure 4.2.** Typical setup for derivation of PML for advective acoustics. Uniform mean flow aligned with the x axis.

## 4.2 Perfectly Matched Layers for Acoustics

The equations of acoustics are obtained by linearizing the Euler equations around a base flow. The uniform base flow  $(\rho_0, u_0, 0, p_0)$ , see Figure 4.2, in two dimensions is often considered in the context of non-reflecting boundary conditions. Here  $(\rho, u, v, p)$  are, perturbations of density, velocity in x and y direction and pressure respectively. For this particular flow the linearized Euler equations can be written as

$$\frac{\partial \mathbf{q}}{\partial t} + A \frac{\partial \mathbf{q}}{\partial x} + B \frac{\partial \mathbf{q}}{\partial y} = 0, \quad (4.7)$$

where the normalization

$$t = \frac{tc_0}{L}, \quad x = \frac{x}{L}, \quad y = \frac{y}{L}, \quad \mathbf{q} = \left[ \frac{\rho}{\rho_0}, \frac{u}{u_0}, \frac{v}{v_0}, \frac{p}{\rho_0 c_0^2} \right]^T,$$

is used to obtain

$$\mathbf{q} = \begin{bmatrix} \rho \\ u \\ v \\ p \end{bmatrix}, \quad A = \begin{bmatrix} M & 1 & 0 & 0 \\ 0 & M & 0 & 1 \\ 0 & 0 & M & 0 \\ 0 & 1 & 0 & M \end{bmatrix}, \quad B = \begin{bmatrix} 0 & 0 & 1 & 0 \\ 0 & 0 & 0 & 0 \\ 0 & 0 & 0 & 1 \\ 0 & 0 & 1 & 0 \end{bmatrix}.$$

Here,  $M = u/c_0$  is the Mach number and  $c_0 = \sqrt{\gamma p_0/\rho_0}$  the speed of sound of the mean flow. Equations (4.7) support three type of waves, sound, entropy, and vorticity waves. Entropy and vorticity waves convect downstream with the mean flow while the two soundwaves travel up or downstream with speed one relative to the mean flow.

For ambient acoustics ( $M = 0$ ), the equations (4.7) become equivalent to the equations describing two dimensional electromagnetics. Hence, stable and well-posed PML formulations are available. For the majority of problems studied in acoustics the flow is advective ( $M \neq 0$ ) and PML formulations derived for computational electromagnetics do not apply directly. Nevertheless, several ideas how to adopt the PML method to the linearized Euler equations have been suggested.

PML for the linearized Euler equations was first derived by Hu in [45]. Using the approach of Berenger, Hu adopted the split field formulation to the Euler equations linearized around an uniform flow pictured in Figure 4.2. Hu later extended his PML to nonuniform flow and to the fully nonlinear Euler equations [46].

In [45] Hu reported that he had to use a low pass filter inside the absorbing layer for the solution to remain stable. Hagstrom and Goodrich reported similar observations in [26]. Later Tam, Auriault and Cambullì [67] proved that the PML devised by Hu supported unstable solutions.

Independently Hesthaven [43], following the analysis in [1], proved that the split PML of Hu was only weakly well-posed. Hesthaven also gave an example of a zero order perturbation leading to unbounded growth.

### 4.2.1 Well-Posed PML for Acoustics

The first well-posed PML for the linearized Euler equations was introduced by Abarbanel, Gottlieb and Hesthaven [3]. They consider isentropic uniform flow for which the linearized Euler equations may be written as (4.7) with

$$\mathbf{q} = \begin{bmatrix} \rho \\ u \\ v \end{bmatrix}, \quad A = \begin{bmatrix} M & 1 & 0 \\ 1 & M & 0 \\ 0 & 0 & M \end{bmatrix}, \quad B = \begin{bmatrix} 0 & 0 & 1 \\ 0 & 0 & 0 \\ 1 & 0 & 0 \end{bmatrix}. \quad (4.8)$$

If  $M = 0$  the equations (4.7) with (4.8) are identical to the T-E mode equations (4.1) and the PML for that problem can be used.

However if  $M \neq 0$ , the dispersion relation becomes much more complicated and the analysis from electromagnetics is not directly applicable. Abarbanel et al. therefore use a transform of variables

$$\xi = x, \quad \eta = \sqrt{1 - M^2}y = \gamma y, \quad \tau = Mx + \gamma^2 t, \quad (4.9)$$

and show that the dispersion relation of the transformed equations is the same as of the T-E mode equations discussed in section 4.1.1. In the transformed variables they derive a PML which only contains zero order perturbations of the equations (4.7) with (4.8), except for one term

$$\frac{\partial Q}{\partial t} = -\gamma^2 \frac{\partial \rho}{\partial y}.$$

By considering the Cauchy problem Abarbanel et al. show that  $Q$  is bounded for all times and therefore the PML is well-posed.

It is interesting to note that the transform of variables (4.9) has been previously used by Bayliss and Turkel [9] and later Hu [47]. In [17], Diaz and Joly use the transformation to construct well-posed PML for the linearized Euler equations.

Recalling the definition used in computational electromagnetics for a stable well-posed PML it is easy to see that the same requirements should hold for a PML for acoustics. I.e. the PML must be absorbing. To analyze the stability of the PML Abarbanel et al. assumed the spatial variations to be small so that they could remove the spatial derivatives in the PML. The resulting system of ordinary differential equations was seen to have solutions growing in time. To remove this growth, they introduced zero order stabilizing profiles which do not alter the well-posedness. But as we shall see below they affect the perfect matching of the PML.

The introduction of the stabilizing profiles was motivated by a separate analysis of a vertical respectively horizontal layer leaving the corners unattended. In [7] we showed that for a simple choice of damping parameters, the PML is unstable in the corners.

Another well-posed PML for the linearized Euler equations for a uniform or parallel flow has been suggested by Hagstrom [38]. The PML suggested by Hagstrom is a direct application of a general way to derive perfectly matched layers for hyperbolic systems in three dimensions described in [38]. In the construction he considers an absorbing layer of width  $L$  at the plane  $x = 0$  with the governing equations (for  $x < 0$ )

$$\frac{\partial u}{\partial t} + A(y) \frac{\partial u}{\partial x} + \sum_j B_j(y) \frac{\partial u}{\partial y_j} + C(y)u = 0, \quad -L < x < 0. \quad (4.10)$$

By Laplace transform in time

$$\hat{u} = e^{\lambda x} \phi, \quad \left( sI + \lambda A + \sum_j B_j(y) \frac{\partial}{\partial y_j} + C(y) \right) \phi = 0, \quad (4.11)$$

it is possible to find the modal solutions to (4.10).

Hagstrom concludes that the solution inside the PML must be modified so that  $\Re \lambda$  is bounded away from zero for  $\Re s \geq 0$ . This guarantees that no generalized eigenvalues, i.e.  $\Re \lambda \rightarrow 0$  as  $\Re s \rightarrow 0$ , are present. Moreover if the eigenfunctions  $\phi$  are the same at the interface  $x = 0$  the absorbing layer will be truly perfectly matched.

Postulating a modal solution inside the PML

$$\hat{u} = e^{\lambda x + (\lambda \hat{R}^{-1} - \hat{M}^{-1} \hat{N}) \int_0^x \sigma(z) dz} \phi, \quad (4.12)$$

and substituting (4.12) into (4.11) gives the resulting PML equations as

$$\left( sI + \lambda A (I - \sigma(\hat{R} + \sigma)^{-1}) \left( \frac{\partial}{\partial x} + \sigma \hat{M}^{-1} \hat{N} \right) + \sum_j B_j(y) \frac{\partial}{\partial y_j} + C(y) \right) \hat{u} = 0.$$

The choice of the operators  $M, N$  and  $R$  is not critical by them self. E.g. Hagstrom suggest that the first two can be chosen as numbers. The question is rather how to choose the combination of them in such a way that all waves are damped. However it is reasonable to choose  $R$  to be a first order, constant coefficient, scalar differential operator in time and in the transverse variables

$$R = \frac{\partial}{\partial t} + \sum_j \beta_j(y) \frac{\partial}{\partial y_j} + \alpha.$$

For the constant coefficient case, the choice of the operators are dictated by an algebraic relation

$$\Re \left( \lambda + \bar{\sigma} \left( \frac{\lambda}{\bar{R}} - \frac{\bar{N}}{\bar{M}} \right) \right) \neq 0, \quad \Re s \geq 0, \quad \bar{\sigma} > 0, \quad (4.13)$$

which is obtained by taking the Fourier transform in the transverse variables. Here, bar denote the transformed version of the operators.

Applying the above analysis to the equations (4.7) and (4.8) the resulting PML is governed by the equations

$$\begin{aligned} \frac{\partial \mathbf{q}}{\partial t} + A \left( \frac{\partial \mathbf{q}}{\partial x} + \mu \sigma \mathbf{q} \right) + B \frac{\partial \mathbf{q}}{\partial y} + \mathbf{w} &= 0, \\ \frac{\partial \mathbf{w}}{\partial t} + \sigma \mathbf{w} + \sigma A \left( \frac{\partial \mathbf{q}}{\partial x} + \mu \sigma \mathbf{q} \right) &= 0. \end{aligned} \quad (4.14)$$

where  $\mathbf{w}$  are auxiliary variables,  $\mu = M/(1 - M^2)$  and  $\sigma$  is the damping profile. Contrary to the PML suggested by Abarbanel et al. the PML (4.14) is truly

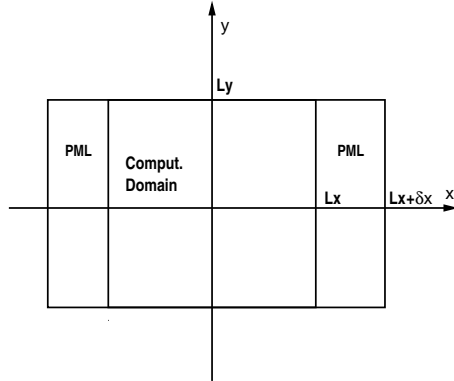


**Figure 4.3.** Computational domain with the added PML, test problem. In computations Mothamed used  $L_x = L_y = 50$ ,  $\delta x = 10$  and  $M = 0.5$ .

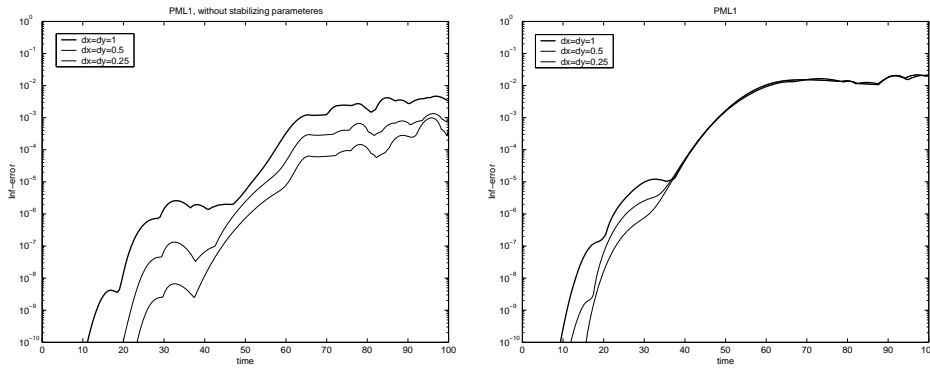
perfectly matched. Abarbanel et al. had suspected that the PML they suggested

was not truly perfectly matched after adding stabilizing parameters but did not investigate if further. In [58] Motamed showed that this indeed is the case.

Motamed compared the PML suggested by Abarbanel et al. with the PML (4.14) for a test problem adopted from [3]. The domain of the test problem is described in Figure 4.3. Inside the computational domain the components  $\rho$ ,  $u$ , and  $v$  were subjected to a continuous forcing. In the  $y$ -direction periodic boundary conditions were used and the PML was terminated by characteristic boundary conditions.

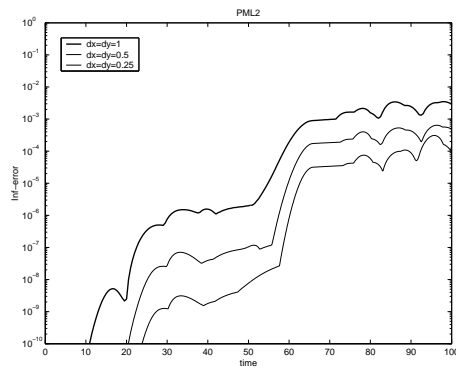
The equations were discretized by second order centered differences in space and advanced in time by the standard fourth order Runge Kutta. The error was measured as the  $L_\infty$ -error along  $x = 48$  using a reference solution computed on a larger domain. Simulations were performed for three successively halved step-sizes.

In Figure 4.4 we see that the  $L_\infty$ -error along the line  $x = 48$  decrease as the resolution is increased for the PML suggested by Hagstrom and also for the PML suggested by Abarbanel et al. if no stabilizing profiles are used. If stabilizing profiles are used in the latter PML the error converges to some fixed value i.e. the PML is not truly perfectly matched.



(a) Error along  $x=48$  for  $\rho$ , Unstabilized PML suggested by Abarbanel et al. If the simulations are performed for longer time the solution will not remain stable.

(b) Error along  $x=48$  for  $\rho$ , Stabilized PML suggested by Abarbanel et al.



(c) Error along  $x=48$  for  $\rho$ , PML suggested by Hagstrom

**Figure 4.4.** All figures are taken from [58].



## Chapter 5

# Summary of Included Papers

### 5.1 Paper I: Evaluation of a Well-posed Perfectly Matched Layer for Computational Acoustics

In this paper we present results from numerical experiments where we solve the linearized Euler equations and use the PML derived in [3] as non-reflecting boundary condition.

The first experiment was conducted to understand why PML for acoustics does not work as well as PML for Maxwell equation. Therefore, we compare the performance of the PML for the two different types of waves, vorticity waves and sound waves, supported by the equations. We also vary the angles of incidence with which the waves approach the boundary. To analyze the result we use a wavesplitting technique to decompose the solution into vorticity and sound waves. The computations show that the PML is less efficient for vorticity waves than for sound waves.

In a second experiment we investigate how the performance of the PML change if it is used as boundary condition for a problem with spatially varying mean flow. Remarkably, the change in performance is small although the PML is not designed for this problem.

We also show, analytically and numerically, that the proposed PML can become unstable for a certain combination of parameters. A stabilizing procedure is proposed and implemented. Numerical results show that the change in performance for the stabilized PML is small.

### 5.2 Paper II: Stabilized Local Non-reflecting Boundary Conditions for High Order Methods

In [61] Rowley and Colonius proposed a discretely non-reflecting boundary condition for computational acoustics. The boundary condition was designed to be

especially efficient for spurious waves introduced by discretization. The boundary condition derived in [61] was derived for an implicit scheme of Padé type. Since different schemes introduce different spurious waves a new discrete boundary condition has to be derived for each scheme.

For many problems appearing in acoustics it is more efficient to use an explicit scheme of high-order, rather than an implicit. In paper II we use the framework introduced by Rowley and Colonius to construct a discretely non-reflecting boundary condition for the one-way wave equation spatially discretized with the standard explicit fourth order accurate difference scheme. The boundary condition, which can be extended to arbitrary order accuracy, is shown to be GKS-stable for orders up to at least 8.

Numerical experiments in one dimension show that the discretely non-reflecting boundary condition outperforms characteristic boundary conditions. Especially for components of the solution that are poorly resolved the derived boundary condition is orders of magnitude better.

The boundary conditions is extended to two space dimensions by combining exact continuous non-reflecting boundary conditions and the one dimensional discretely non-reflecting boundary condition. The resulting boundary condition is localized by the standard Padé approximation. By using auxiliary variables the two dimensional boundary condition can, in principal, be extended to high-order. However it is found by numerical experiments that the resulting method suffers from *boundary instabilities*.

Analysis of a related continuous problem suggests that the discrete boundary condition can be stabilized by adding tangential viscosity at the boundary. For the lowest order Padé approximation we are able to stabilize the discrete boundary condition. However, the results of the stabilized boundary condition is not satisfactory. The reflections are smaller than for the characteristic boundary condition but does not motivate the extra work needed to implement them.

# Bibliography

- [1] S. Abarbanel and D. Gottlieb. A mathematical analysis of the pml method. *J. Comput. Phys.*, (134):357, 1997.
- [2] S. Abarbanel and D. Gottlieb. On the construction and analysis of absorbing layers in cem. *Appl. Numer. Math.*, (27):331, 1998.
- [3] S. Abarbanel, D. Gottlieb, and J.S Hesthaven. Well-posed perfectly matched layers for advective acoustics. *J. Comput. Phys.*, 154:266–283, 1999.
- [4] S. Abarbanel, D. Gottlieb, and J.S Hesthaven. Long time behaviour of the perfectly matched layer equations in computational electromagnetics. *J. Sci. Comput.*, 17(1-4):405–422, 2002.
- [5] B. Alpert, L. Greengard, and T. Hagstrom. Rapid evaluation of nonreflecting boundary kernels for time-domain wave propagation. *SIAM J. Numer. Anal.*, 37(4):1138–1164, 2000.
- [6] B. Alpert, L. Greengard, and T. Hagstrom. Nonreflecting boundary conditions for the time dependent wave equation. *J. Comput. Phys*, 180:270–296, 2002.
- [7] D. Appelö and G. Kreiss. Evaluation of a well-posed perfectly matched layer for computational acoustics. In T.Y. Hou E. Tadmor, editor, *Hyperbolic Problems: Theory, Numerics, Applications, Proceedings of the Ninth International Conference on Hyperbolic Problems*, pages 285–294. Springer Verlag, 2002.
- [8] S. Asvadurov, V. Druskin, M.N. Guddati, and L. Knizhnerman. On optimal finite-difference approximation of pml. *SIAM J. Numer. Anal.*, 41:287–305, 2003.
- [9] A. Bayliss and E. Turkel. Radiation boundary conditions for wave-like equations. *Comm. Pure Appl. Math.*, 33:707, 1980.
- [10] E. Bècache and P. Joly. On the analysis of brenger’s perfectly matched layers for maxwell’s equations. *Math. Mod. Numer. Anal.*, 36(1):87–119, 2002.

- [11] E. Bècache, P.G. Petropoulos, and S.D. Gedney. Long-time behavior of the unsplit pml. In E. Heikkola P. Neittaanmki G.C. Cohen, P. Joly, editor, *Mathematical and Numerical Aspects of Wave Propagation, Proceedings Waves2003*, pages 120–124. Springer Verlag, 2003.
- [12] J. Berenger. A perfectly matched layer for the absorption of electromagnetic waves. *Journal of Computational Physics*, 114:185, 1994.
- [13] F. Collino. High order absorbing boundary conditions for wave propagation models. straight line boundary and corner cases. In R. Kleinman and et al., editors, *Proceedings of the 2nd International Conference on Mathematical and Numerical Aspects of Wave Propagation*, pages 161–171. SIAM, Delaware, 1993.
- [14] F. Collino. Perfectly matched absorbing layers for the paraxial equations. *J. Comput. Phys.*, 113:164–180, 1997.
- [15] F. Collino and P. Monk. Optimizing the perfectly matched layer. *SIAM J. Sci. Comp.*, 19:2061–2090, 1998.
- [16] T. Colonius. Modeling artificial boundary conditions for compressible flow. draft version, 2003.
- [17] J. Diaz and P. Joly. Stabilized perfectly matched layer for advective acoustics. In E. Heikkola P. Neittaanmki G.C. Cohen, P. Joly, editor, *Mathematical and Numerical Aspects of Wave Propagation, Proceedings Waves2003*, pages 115–119. Springer Verlag, 2003.
- [18] B. Engquist and A. Majda. Absorbing boundary conditions for the numerical simulation of waves. *Math. Comp.*, 31:629, 1977.
- [19] A. Ergin, B. Shanker, and E. Michielssen. Fast evaluation of three-dimensional transient wave fields using diagonal translation operators. *J. Comput. Phys*, 146:157–180, 1998.
- [20] K. Gerdes. A review of infinite element methods for exterior helmholtz problems. *J. Comput. Acoust.*, 8(1):43–62, 2000.
- [21] M. Giles. Nonreflecting boundary conditions for euler equation calculations. *AIAA Journal*, 28:2050–2058, 1990.
- [22] D. Givoli. Non-reflecting boundary conditions a review. *J. Comput. Phys*, 94:1–29, 1991.
- [23] D. Givoli. High-order nonreflecting boundary conditions without high-order derivatives. *J. Comput. Phys*, 170:849–870, 2001.
- [24] D. Givoli and D. Cohen. Non-reflecting boundary conditions based on kischoff-type formulae. *J. Comput. Phys.*, 117:102–113, 1995.

- [25] D. Givoli and B. Neta. High-order non-reflecting boundary scheme for time-dependent waves. *J. Comput. Phys.*, 186:24–46, 2003.
- [26] J.W. Goodrich and T. Hagstrom. A comparison of two accurate boundary treatments for computational aeroacoustics. Technical Report 97-1585, AIAA, 1999.
- [27] J.W. Goodrich and T. Hagstrom. Accurate radiation boundary conditions for the linearized euler equations in cartesian domains. *to appear*, 2003.
- [28] M. Grote. Non-reflecting boundary conditions for electromagnetic scattering. *Int. J. Numer. Model.*, (13):397–416, 2000.
- [29] M. Grote. Nonreflecting boundary conditions for elastodynamic scattering. *J. Comput. Phys.*, (161):331–353, 2000.
- [30] M. Grote and J. Keller. Exact nonreflecting boundary conditions for the time dependent wave equation. *SIAM J. Appl. Math.*, (55):280–297, 1995.
- [31] M. Grote and J. Keller. Nonreflecting boundary conditions for time dependent scattering. *J. Comput. Phys.*, 127:52–81, 1996.
- [32] M. Grote and J. Keller. Nonreflecting boundary conditions for maxwell’s equations. *J. Comput. Phys.*, (139):327–324, 1998.
- [33] M. Grote and J. Keller. Nonreflecting boundary conditions for elastic waves. *SIAM J. Appl. Math.*, (60):803, 2000.
- [34] M.N. Guddati and J.L Tassoulas. Continued-fraction absorbing boundary conditions for the wave equation. *J. Comp. Acoust.*, 8(1):139–156, 2000.
- [35] T. Hagstrom. On high-order radiation boundary conditions in. In B. Engquist and G. Kriegsmann, editors, *IMA Volume on Computational Wave Propagation*, pages 1–22. Springer, New York, 1996.
- [36] T. Hagstrom. Progressive wave expansions and open boundary problems. In B. Engquist and G. Kriegsmann, editors, *IMA Volume on Computational Wave Propagation*, pages 23–43. Springer, New York, 1996.
- [37] T. Hagstrom. Radiation boundary conditions for the numerical simulation of waves. *Acta. Numer.*, 8:47–106, 1999.
- [38] T. Hagstrom. New results on absorbing layers and radiation boundary conditions. preprint, 2003.
- [39] T. Hagstrom and S.I. Hariharan. A formulation of asymptotic and exact boundary conditions using local operators. *Appl- Numer. Math.*, 27:403–416, 1998.

- [40] L. Halpern and L.N. Trefethen. Wide-angle one-way wave equations. *J. Acoust. Soc. Am.*, 84:1397–1404, 1988.
- [41] E. Harrier, C. Lubich, and M. Schlichte. Fast numerical solution of nonlinear volterra convolutional equations. *SIAM J. Sci. Stat. Comput.*, 6:532–541, 1985.
- [42] D. Healy, D. Rockmore, P. Kostelec, and S. Moore. Ffts for the 2-sphere, improvements and variations. *Adv. Appl. Math.*, 2002 to appear.
- [43] J.S. Hesthaven. On the analysis and construction of perfectly matched layers for the linearized euler equations. *J. comput. Phys.*, 142:129–147, 1998.
- [44] R.L. Higdon. Absorbing boundary conditions for difference approximations to the multidimensional wave equation. *Math. Comp.*, 47:437–459, 1986.
- [45] F. Q. Hu. On absorbing boundary conditions for linearized euler equations by a perfectly matched layer. *J. Comput. Phys.*, 129:201–209, 1996.
- [46] F. Q. Hu. On perfectly matched layer as a boundary condition. Technical Report 96-1664, AIAA, 1996.
- [47] F. Q. Hu. A stable perfectly matched layer for linearized euler equations in unsplit physical variables. *J. Comput. Phys.*, 173:455–480, 2001.
- [48] R. Huan and L.L. Thompson. Accurate radiation boundary conditions for the time-dependent wave equation on unbounded domains. *Int. J. Numer. Meth. Engrg.*, 47:1569–1603, 2000.
- [49] M. Israeli and S.A. Orzag. Approximation of radiation boundary conditions. *J. Comput. Phys.*, 41:115–135, 1981.
- [50] S. Karni. Far-field filtering operators for supression of reflections of artificial boundaries. *SIAM J. Numer. Anal.*, 33:1014–1047, 1996.
- [51] R. Kosloff and D. Kosloff. Absorbing boundaries for wave propagation problems. *J. Comput. Phys.*, 63:363–376, 1986.
- [52] H-O. Kreiss and J. Lorenz. *Initial-Boundary Value Problems and the Navier-Stokes Equations*. Academic Press Inc., 1989.
- [53] M. Lassas, J. Liukkonen, and E. Somersalo. Complex riemannian metric and absorbing boundary conditions. *J. Math. Pures Appl.*, 80(7):739–768, 2001.
- [54] E. L. Lindman. "free space" boundary conditions for the time dependent wave equation. *J. Comput. Phys.*, 18:66–78, 1975.
- [55] J.L. Lions, J. Metral, and O. Vacus. Well-posed absorbing layer for hyperbolic problems. *Numer. Math.*, 92:535–562, 2002.

- [56] C. Lubich and M. Schlichte. Fast convolution for nonreflecting boundary conditions. *SIAM J. Sci. Comput.*, 24(1):161–182, 2002.
- [57] M. Mohlenkamp. A fast transform for spherical harmonics. *J. of Fourier Anal. and Applic.*, 5:159–184, 1999.
- [58] M. Motamed. Pml methods for aero acoustics computations. Master’s thesis, KTH, 2003.
- [59] P.G. Petropoulos. Reflectionless sponge layers as absorbing boundary conditions for the numerical solution of maxwell equations in rectangular, cylindrical and spherical coordinates. *SIAM J. Appl. Math.*, 60(3):1037–1058, 2000.
- [60] A. Ramm. *Scattering by obstacles*. D. Reidel, Dordrecht, Netherlands, 1986.
- [61] C. W. Rowley and T. Colonius. Discretely nonreflecting boundary conditions for linear hyperbolic systems. *J. Comput. Phys.*, 157:500–538, 2000.
- [62] V.S. Ryaben’kii, S.V. Tsynkov, and V.I. Turchaninov. Global discrete artificial boundary conditions for time dependant wave propagation. *J. Comput. Phys.*, 174:712–758, 2001.
- [63] I. Sofronov. Conditions for complete transparency on the sphere for the three dimensional wave equation. *Russian Acad. Sci. Dokl. Math.*, (46):397–401, 1993.
- [64] I. Sofronov. Artificial boundary conditions of absolute transparency for two- and three-dimensional external time-dependent scattering problems. *Euro. J. Appl. Math.*, (9):561–588, 1998.
- [65] R. Suda and M. Takami. A fast spherical harmonics transform algorithm. *Math. Comp.*, (71):703–715, 2002.
- [66] A. Taflove. *Computational Electromagnetics The Finite-Difference Time-Domain Method*. Artech House, 1995.
- [67] C. K. W. Tam, L. Auriault, and F. Cambuli. Perfectly matched layer as an absorbing boundary condition for the linearized euler equations in open and ducted domains. *J. Comput. Phys.*, 144:213–234, 1998.
- [68] L.L. Thompson and R. Huan. Implementation of exact non-reflecting boundary conditions in the finite element method for the time-dependent wave equation. *Comput. Meth. Appl. Mech. Engrg.*, 187:137–159, 2000.
- [69] L. Ting and M.J. Miksis. Exact boundary conditions for scattering problems. *J. Acoust. Soc. Amer.*, 80:1825–1827, 1986.
- [70] L.N. Trefethen and L. Halpern. Well-posedness of one-way wave equations and absorbing boundary conditions. *Math. Comp.*, 176:421–435, 1986.

- [71] S.V. Tsynkov. Numerical solution of problems on unbounded domains, a review. *Appl. Numer. Math.*, 27:465–532, 1998.
- [72] E. Turkel and A. Yefet. Absorbing pml boundary layers for wave-like equations. *Appl. Numer. Math.*, 27:533–557, 1998.
- [73] L. Zhao and A.C. Cangellaris. Gt-pml: Generalized theory of perfectly matched layers and its application to reflectionless truncation of finite-difference time-domain grids. *IEEE Trans. Microwave Theory Tech.*, 44:2555–2563, 1996.
- [74] R. Ziolkowski. Time-derivative lorenz-material model based absorbing boundary condition. *IEEE Trans. Antennas Propagation*, 45:1530–1535, 1997.

# Evaluation of a well-posed Perfectly Matched Layer for Computational Acoustics

Daniel Appelö<sup>1</sup> and Gunilla Kreiss<sup>1</sup>

<sup>1</sup> NADA, KTH, Sweden [appelo@nada.kth.se](mailto:appelo@nada.kth.se)

<sup>2</sup> NADA, KTH, Sweden [gunillak@nada.kth.se](mailto:gunillak@nada.kth.se)

## 1 Introduction

Accurate numerical simulations of wave phenomena are important in many fields, for example in electro magnetics, seismics and acoustics. We are interested in aeroacoustic problems with a non-vanishing mean flow. The governing equations are the Euler equations. In a typical aeroacoustic situation the solution consists of a slowly varying mean flow with an added small amplitude acoustic wave.

The simulations must in general be confined to truncated domains, much smaller than the physical space where the phenomena takes place. At the artificial boundary, where the truncation takes place, boundary conditions must be set. Ideally the solution of the problem in the truncated domain is identical to the solution of the original problem. However, often undesirable effects, such as reflections, limit the accuracy of the solution of the truncated problem. Boundary conditions that do not cause reflections are called absorbing or non-reflecting boundary conditions

Some of the earliest absorbing or non-reflecting boundary conditions were derived for the wave equation by Engquist and Majda [6] and Bayliss and Turkel [4]. For an overview of the subsequent development of absorbing boundary conditions for wave propagation problems, see for instance Hagstrom [8].

For Maxwell's equations an important advance is the derivation of perfectly matched layers (PML) by Berenger [5] in 1994. The idea of the PML is to surround the computational domain with an highly absorbing layer in which the outgoing waves is attenuated. The governing equations of the absorbing layer must be matched with the equations of the computational domain, i.e. there should be no reflection at the interface of incoming waves, independent of their angle of incidence and frequency. Berenger introduced a splitting of the equations to obtain the additional degrees of freedom needed to match the equations at the interface. The resulting PML was orders of magnitude better than earlier Absorbing Boundary conditions (ABC's). One serious disadvantage of Berengers PML, discovered by Abarbanel and Gottlieb [1], was that the splitted set of PDE's was only weakly well-posed. Other derivations of a PML for Maxwell's equations which are well-posed have been presented [2], and are as efficient as Berengers PML. Today PML is commonly used in commercial CEM software.

In 1996 Hu [10] derived a PML for the Euler equations, linearized at constant flow, by using the splitting technique introduced by Berenger. An analysis of this PML showed that it is only weakly well-posed[9]. In 1998 Abarbanel, Gottlieb and Hesthaven [3] derived a well-posed PML. However, the PML technique has so far not been as succesfull for the linearized Euler equations as for the Maxwells equations. This is true even in the case of vanishing mean flow. One difference, which may be important is the presence of vorticity waves.

In this paper we present results from numerical experiments where we solve the linearized Euler equations and use the PML derived in [3] as ABC.

In one experiment we compare the performance of the PML for the two different types of waves, vorticity waves and sound waves, that are supported by the equations. We have also varied the angles of incidence with which the waves approach the boundary. To analyze the result we use the wavesplitting technique of Wilson [7], described in Jensen, Efraimsson [11], to decompose the solution into the different waves. The computations show that the PML is less efficient for vorticity waves than for sound waves.

In an other experiment we vary the mach number spatially. Computations show that varying Mach number does not effect the performance of the PML significantly.

## 2 The PML and test problems

The PML in [3] is derived for the Euler equations linearized around an isentropic uniform (aligned to the  $x$ -axis) flow on a rectangular domain represented in Cartesian coordinates. The equations are nondimensionalized with the Mach number  $M$ . In all cases with constant  $M$  we have used  $M = 0.5$ . The PML is derived in a transformed coordinate system. The transformation  $(x, y, t) \rightarrow (\xi, \eta, \tau)$  is defined by

$$\xi = x, \quad \eta = \sqrt{1 - M^2}y = \gamma y, \quad \tau = Mx + \gamma^2 t. \quad (1)$$

Eigenvalues belonging to plane wave solutions of the transformed problem satisfy a simple dispersion relation which simplifies the derivation of the PML. The derivation is done separately for the  $\xi$ - and  $\eta$ -direction, resulting in two sets of well-posed perfectly matched layers, which are added together, overlapping each other in the corners. The PML is transformed back to the physical coordinate system  $(x, y, t)$  yielding,

$$\begin{aligned}
 \frac{\partial v}{\partial t} + M \frac{\partial v}{\partial x} + \frac{\partial \rho}{\partial y} &= -\sigma_x v + 2\sigma_x Q_x + \sigma_x^2 R_x + M\sigma_x' P_x \\
 &\quad + 2\sigma_y Q_y + \sigma_y^2 R_y + \sigma_y' P_y - \varepsilon_x v + 2\mu_y Q_y, \\
 \frac{\partial u}{\partial t} + M \frac{\partial u}{\partial x} + \frac{\partial \rho}{\partial x} &= -\sigma_x u - \sigma_x M \rho - \mu_y u, \\
 \frac{\partial \rho}{\partial t} + M \frac{\partial \rho}{\partial x} + \frac{\partial u}{\partial x} + \frac{\partial v}{\partial y} &= -\sigma_x \rho - \sigma_x M u - \mu_y \rho, \\
 \frac{\partial Q_x}{\partial t} &= -\gamma^2 \frac{\partial \rho}{\partial y}, \\
 \frac{\partial Q_y}{\partial t} &= \gamma^2 \frac{\partial \rho}{\partial y} - 2\sigma_y Q_y - \sigma_y^2 R_y - \sigma_y' P_y + \sigma_x v \\
 &\quad - 2\sigma_x Q_x - \sigma_x^2 R_x - M\sigma_x' P_x + \mu_x v - 2\mu_y Q_y, \\
 \frac{\partial P_x}{\partial t} &= \gamma^2 [v - \sigma_x P_x - \varepsilon_x P_x], \\
 \frac{\partial P_y}{\partial t} &= \gamma^2 [\rho - \sigma_y P_y], \\
 \frac{\partial R_x}{\partial t} &= \gamma^2 [Q_x - \mu_x R_x], \\
 \frac{\partial R_y}{\partial t} &= \gamma^2 [Q_y - \mu_y R_y].
 \end{aligned} \tag{2}$$

The parameters  $\sigma_x = \sigma_x(x)$  and  $\sigma_y = \sigma_y(y)$  are polynomials starting at zero at the PML-interface and monotonically increasing through the PML. By setting the parameters  $\sigma_x$  and  $\sigma_y$  to zero the linearized Euler equations are recovered for the velocity components  $u$  and  $v$  and the density  $\rho$ .

The parameters  $\varepsilon_x$ ,  $\mu_x$  and  $\mu_y$  are added to the PML to prevent algebraic growth. They are motivated in [3] by an analysis of a system of ODE's obtained by neglecting spatial variations. In chapter 3 we show that the addition of  $\varepsilon_x$ ,  $\mu_x$  and  $\mu_y$  is insufficient to prevent growing solutions. We also suggest an ad hoc modification of the PML that prevent growing solutions.

## 2.1 Testproblem 1

The first test problem is adopted from [3]. The computational domain is bounded by  $|x| \leq L_x, |y| \leq L_y$ , we choose  $L_x = L_y = 50$ . Outside the computational domain a PML of thickness  $\delta_x, \delta_y$  respectively is added. The PML is terminated with characteristic boundary conditions. In the inner domain, the linearized Euler equations are solved, and in the outer domain the PDE's (2). In the inner domain  $\rho, u$  and  $v$  are subjected to a continuous forcing

$$\begin{aligned}
\rho^f(x, y, t) &= e^{-(\ln 2) \frac{(x-x_a)^2 + (y-y_a)^2}{\delta_a^2}} \sin\left(\frac{\pi t}{10}\right), \\
u^f(x, y, t) &= 0.05(y - y_b) e^{-(\ln 2) \frac{(x-x_b)^2 + (y-y_b)^2}{\delta_b^2}} \sin\left(\frac{\pi t}{10}\right), \\
v^f(x, y, t) &= -0.05(x - x_b) e^{-(\ln 2) \frac{(x-x_b)^2 + (y-y_b)^2}{\delta_b^2}} \sin\left(\frac{\pi t}{10}\right),
\end{aligned} \tag{3}$$

where  $(x_a, y_a)$  is the center of the sound source, which has the width  $\delta_a$ ,  $(x_b, y_b)$  is center of the vorticity source with width  $\delta_b$ . The centers and widths are  $(x_a, y_a) = (-25, 0)$ ,  $(x_b, y_b) = (25, 0)$ ,  $\delta_a = 3$ ,  $\delta_b = 4$  respectively. The error is measured as the  $l_2^2$  error along the line  $x = 48$ . For testproblem 1 the PML thickness  $\delta_x$  and  $\delta_y$  are varied. The testproblem is extended to include spatially varying mach number. This is discussed in section 4.

## 2.2 Wavesplitting

Let  $\mathbf{f} = [\rho, u, v]^T$ . By Fourier transform the function  $\mathbf{f}$  can be represented as  $\hat{\mathbf{f}}(x, k_y, \omega) = \mathcal{F}\{\mathbf{f}(x, y, t)\}$  and then the linearized Euler equations may be written as

$$\mathbf{A} \frac{\partial \hat{\mathbf{f}}}{\partial x} + \mathbf{B}(x, i_k y, i\omega) \hat{\mathbf{f}} = 0. \tag{4}$$

The eigenvectors of the matrix  $\mathbf{A}^{-1}\mathbf{B}$  form the columns of the matrix  $\mathbf{L}$  used to define  $\mathbf{q} = \mathbf{L}^{-1}\hat{\mathbf{f}}$ . After multiplying (4) with  $\mathbf{A}^{-1}$  and  $\mathbf{L}^{-1}$  we obtain the decoupled system of ordinary differential equations

$$\frac{\partial \mathbf{q}}{\partial x} + \mathbf{\Lambda} \mathbf{q} = 0,$$

where  $\mathbf{\Lambda} = \text{diag}([\lambda_{ds}, \lambda_{us}, \lambda_{vor}])$  contains the eigenvalues of  $\mathbf{A}^{-1}\mathbf{B}$ . The absolute value of the components of  $\mathbf{q}$  are the amplitudes of the upstream and downstream sound wave and the vorticity wave.

## 2.3 Testproblem 2

The second testproblem is adopted from [11]. The test problem is designed to test the efficiency of an absorbing boundary condition for down-stream sound wave and vorticity wave, separately.

The computational domain is  $0 < x < L_x$ ,  $|y| < L_y$ . At  $x = 0$  we prescribe the solution and at  $x = L_x$  we use PML terminated with characteristic boundary conditions. In the y-direction we use periodic boundary conditions.

By using the wavesplitting technique, described above, we derive boundary conditions for the inflow-boundary that corresponds to either a pure

downstream plane sound wave solution or a pure vorticity plane-wave solution with amplitude 1.

Fixing the height of the computational domain to  $|y| \leq L_y = 50$  and the wave number  $k_y = 2\pi/100$  the solution is periodic in the y-direction. By specifying different frequencies  $\omega$  we obtain plane wave solutions which propagate in different angles relative the y-axis. The width of the computational domain,  $L_x$ , is chosen such that one period of the solution is contained within. Further we use  $\delta_x = L_x$ .

## 2.4 Discretization

To simulate the testproblems we have used standard 2:nd order central differences in space and 4:th order Runge-Kutta to advance in time. In [3] a 4:th order scheme is used in space but for our evaluation this difference is not significant. For testproblem 2, since the exact solution was known, the discretization step was chosen to be 25 points per wavelength both in space and time. In testproblem 1 the discretization step was chosen empirically so that the computed solution was well resolved in space and time.

## 3 Analysis of corners

During simulations of the first testproblem using the discretization described above we experienced growth originating from the corners. To understand the growth we consider (2) with  $\sigma_x$  and  $\sigma_y$  constant and  $\varepsilon_x = \mu_x = \mu_y = 0$  to obtain a constant coefficient problem.

Using the notation  $w = [v, u, \rho, Q_x, Q_y, P_x, P_y, R_x, R_y]^T$  we write (2) as

$$\frac{\partial w}{\partial t} = A \frac{\partial w}{\partial x} + B \frac{\partial w}{\partial y} + Cw. \quad (5)$$

By Fourier transform in the x and y directions we obtain

$$\frac{\partial \hat{w}}{\partial t} = (i\xi A + i\eta B + C)\hat{w} \equiv \mathbf{P}(i\xi, i\eta, t)\hat{w}.$$

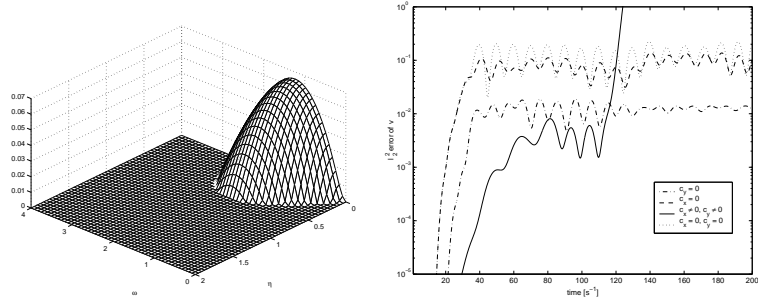
Here  $\mathbf{P}$  is a  $9 \times 9$  matrix. If the eigenvalues of  $\mathbf{P}(i\xi, i\eta, t)$  have real part greater than zero  $\|w\|$  will grow. To investigate this we numerically calculate the eigenvalues  $\lambda_i$  of  $\mathbf{P}$  for fixed  $\xi$  and  $\eta$ .

Let  $\lambda_{max} = \max[\text{Re}\{\lambda_i\}]$ . In figure 1(a)  $\lambda_{max}$  is plotted for a set of frequencies. Clearly there exist  $\lambda_{max} > 0$ , explaining the growth experienced.

To investigate whether the analysis of the constant coefficient system (5) is relevant for the first testproblem we calculated  $\lambda_{max}$  for the spatial discretisation of (2) including non constant  $\sigma_x$  and  $\sigma_y$  and choosing the parameters  $\mu_x$ ,  $\mu_y$  and  $\varepsilon_x$  according to [3]. Also for this case  $\lambda_{max} > 0$ . This result was

obtained independent of the discretization step size. The growth rate of the norm of the solution could be connected to  $\lambda_{max}$ .

Investigation of the eigenfunctions, corresponding to growing modes, showed that they were nonzero only at nodes where  $\sigma_x$  and  $\sigma_y$  were simultaneously nonzero, i.e. in the corners. The simplest way to get rid of the growth



(a) Plot of  $\text{Re}\{\lambda_{max}\}$  for some frequencies. The bump corresponds to growing modes.

(b) Exponential growth for overlapping  $\sigma_x$  and  $\sigma_y$ , no growth with the suggested fix. The decrease in efficiency is about one half order of magnitude. Here  $c_i = \sigma_i$ .

**Fig. 1.**

was to prevent  $\sigma_x$  and  $\sigma_y$  from being simultaneously nonzero. This can be accomplished by putting either  $\sigma_x$  or  $\sigma_y$  or both zero in the corners where they overlap. In figure 1(b) performance for the three different choices and the original setup is shown.

The best choice seems to be keeping the PML at the in and outflow boundaries intact and putting  $\sigma_y = 0$  inside that PML (the dash-dotted line). Note that the error level of the modified PML is only one half order of magnitude worse than the original. The modified approach has been integrated for long time and no growth have been seen.

## 4 Numerical results

### 4.1 Variable machnumber

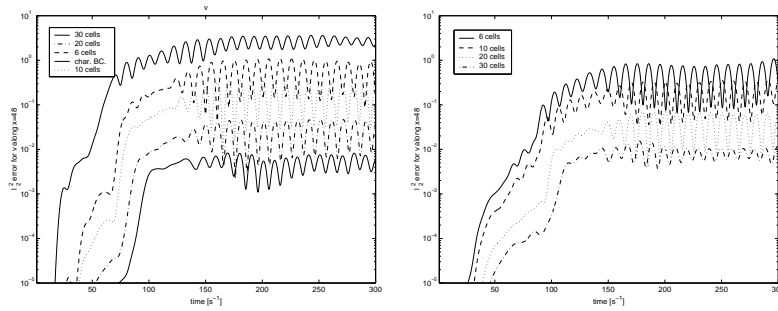
To make an acoustic ABC practically useful it should be applicable to the linearized Euler equations with variable mach number and hopefully to the

Euler equations. We have considered the simpler of these two extensions by making experiments on a case where we let the machnumber vary spatially. A spatial variation of the machnumber may be used in simulations of acoustic waves in nozzles or subsonic jets.

We have made computations for a spatially varying machnumber,

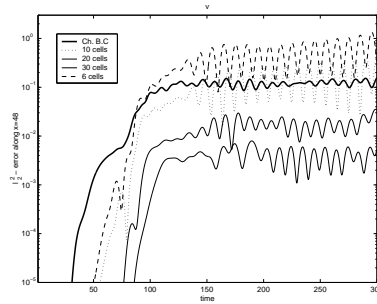
$$M = M(z) = e^{\frac{-z^2}{10^2}}, \quad \text{where } z \text{ is either } x \text{ or } y. \quad (6)$$

The performance of the PML for these two cases seems to be nearly as good as for the constant mach number (compare figures 2(a)-2(c)). We conclude that the PML may be used for this kind of computations.



(a) Error along  $x=48$  for  $v$  for constant Machnumber

(b) Error along  $x=48$  for  $v$  for a simulated subsonic jet



(c) Error along  $x=48$  for  $v$  for a simulated slim nozzle

**Fig. 2.** The difference in performance for spatially varying Machnumber compared to constant is small. It should be noted that the form of the curves for the error coincides with [3] but the level is higher.

## 4.2 Efficiency for different waves

We used zero as initial condition for testproblem 2. To avoid transient noise the solution was first integrated in time for 100 periods. After that the solution was integrated and saved for another period.

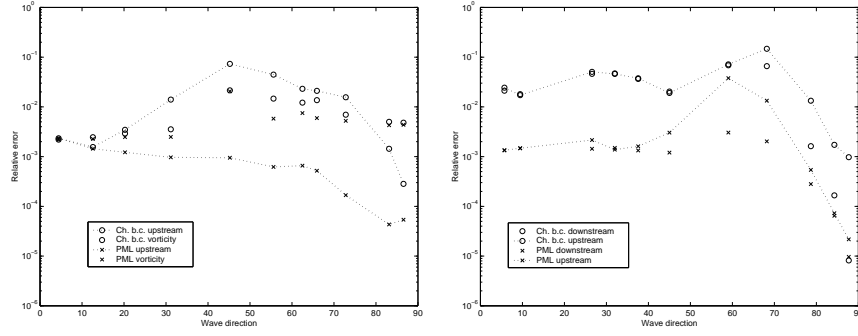
**Fourier transforming and wavesplitting.** To compare different numerical solutions we use the Fourier transform in time and in the y-direction. We then use the wavesplitting technique (described above) to extract separate information on each of the waves of the solution. For each node in the x-direction the amplitude of the other two waves (which ideally should be zero) gives an estimate of the relative error in the computed solution.

In figures 4(a) - 5(b) some examples are shown. We like to stress that in all tests the upstream soundwave amplitude should be taken as the significant estimate of the performance of the absorbing boundary condition since it is the only one which is reflected from the PML. The other wave is due to the boundary treatment at the inflow boundary.

The results in figures 3(a) and 3(b) show that the PML performs best for waves which fall in normal to the outflow boundary. For soundwaves the performance deteriorates as the angle of incidence decreases. Surprisingly for vorticity waves the worst performance is found at an angle of 60 degrees. However the efficiency of the PML for different angles is always better than characteristic boundary conditions.

## References

1. S. Abarbanel and D. Gottlieb. A mathematical analysis of the pml method. *J. Comput. Phys.*, 134:357, 1997.
2. S. Abarbanel and D. Gottlieb. On the construction and analysis of absorbing layers in cem. *Appl. Numer. Math.*, 27:331, 1998.
3. S. Abarbanel, D. Gottlieb, and J.S Hesthaven. Well-posed perfectly matched layers for advective acoustics. *Journal of Computational Physics*, 154:266–283, 1999.
4. A. Bayliss and E. Turkel. Radiation boundary conditions for wave-like equations. *Comm. Pure Appl. Math.*, 33:707, 1980.
5. J. P. Brernger. A perfectly matched layer for the absorption of electromagnetic waves. *Journal of Computational Physics*, 114:185, 1994.
6. B. Engquist and A. Majda. Absorbing boundary conditions for the numerical simulation of waves. *Math. Comp.*, 31:629, 1977.
7. Wilson. A. G. Method for deriving tone noise information from cfd calculations on the aeroengine fan stage. draft paper, RollsRoyce plc, United Kingdom, 2000.
8. Thomas Hagstrom. Radiation boundary conditions for the numerical simulation of waves. *Acta Numerica*, pages 47–106, 1999.
9. J.S. Hesthaven. On the analysis and construction of perfectly matched layers for the linearized euler equations. *Journal of computational Physics*, 142:129–147, 1998.

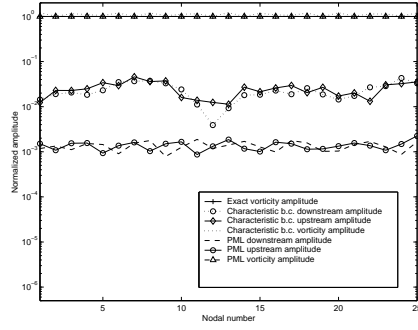


(a) *Downstream soundwave.* The curves display the mean relative error for the vorticity and upstream soundwave. Note that the PML is better than ch. b.c. for all angles except for almost glancing incidence where the ch. b.c. seems to perform as well.

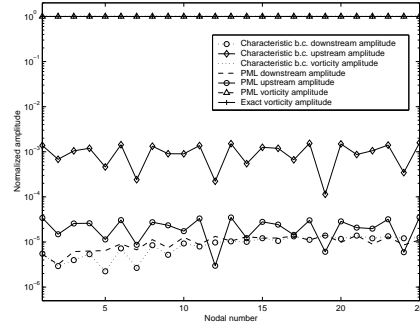
(b) *Vorticity wave.* Mean relative error for the vorticity and upstream soundwave. For this type of inflow b.c. the PML is better at all angles.

**Fig. 3.** The comparison between vorticity and soundwaves show that the PML work better for the soundwaves since the vorticity waves has a dip in performance at 60 degree. The error displayed on the y-axis is the mean error over all x-nodes in the computational domain.

10. F. Q. Hu. On absorbing boundary conditions for linearized euler equations by a perfectly matched layer. *Journal of Computational Physics*, 129:201–209, 1996.
11. Kristoffer Jensen and Gunilla Efraimsson. Aeroengine fan-noise resolution requirement in computational fluid dynamics. Technical report, Swedish Defence research agency, FOI, 2001.

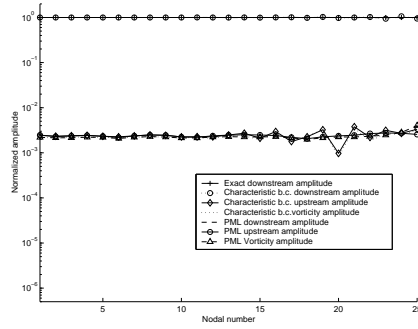


(a) Vorticity wave incoming at angle 5.7 degree (almost glancing incidence).

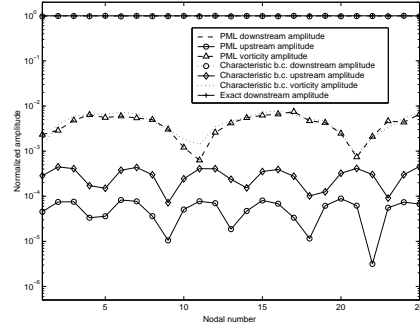


(b) Vorticity wave incoming at angle 87.7 degree (almost normal incidence).

**Fig. 4.** Comparison between PML and characteristic boundary condition for a Vorticity wave along the computational domain. Note that both boundary conditions work best at normal incidence.



(a) Downstream soundwave incoming at angle 4.4 degree (almost glancing incidence).



(b) Downstream soundwave incoming at angle 86.6 degree (almost normal incidence).

**Fig. 5.** Comparison between PML and characteristic boundary condition for a downstream soundwave. Note that both boundary conditions work best at normal incidence.



KUNGL  
TEKNISKA  
HÖGSKOLAN



Department of Numerical Analysis and Computer Science  
TRITA-NA-0325 • ISSN 0348-2952 • ISRN KTH/NA/R--03/25--SE

---

# **Stabilized Local Non-reflecting Boundary Conditions for High Order Methods**

**Daniel Appelö and Gunilla Kreiss**

**Numerical Analysis**

Daniel Appelö and Gunilla Kreiss

*Stabilized Local Non-reflecting Boundary Conditions for High Order Methods*

Report number: TRITA-NA-0325, ISRN KTH/NA/R--03/25--SE

Publication date: November 2003

E-mail of author: [appelo@nada.kth.se](mailto:appelo@nada.kth.se)

Department of Numerical Analysis and Computer Science

Royal Institute of Technology

SE-100 44 Stockholm

SWEDEN

## Abstract

Using the framework introduced by Rowley and Colonius [14] we construct a discretely non-reflecting boundary condition for the one-way wave equation spatially discretized with an explicit fourth order centered difference scheme. The boundary condition, which can be extended to arbitrary order accuracy, is shown to be GKS-stable. We continue by deriving discretely non-reflecting boundary conditions for systems in two dimensions using the results for the scalar one dimensional case.

TRITA-NA-0325 • ISSN 0348-2952 • ISRN KTH/NA/R--03/25--SE



# 1 Introduction

When solving hyperbolic problems numerically on unbounded domains, the problem is confined to a smaller computational domain by introducing an artificial boundary. For many hyperbolic problems the correct boundary condition is that waves traveling across the boundary should not be reflected back. Boundary conditions which prevent waves from being reflected are often referred to as non-reflecting boundary conditions. Sometimes they may be referred to as transparent, artificial or absorbing boundary conditions.

Non-reflecting boundary conditions have been a matter of research for many decades. Some early explorers of the area were Lindeman [13] and Engquist and Majda [4], [5], who derived non-reflecting boundary conditions for the scalar wave equation. The works of Engquist and Majda have been an important source of inspiration in the construction of non-reflecting boundary conditions in different fields.

Boundary conditions of Engquist - Majda type are often formulated as a sequence of partial differential equations (PDE) which do not allow waves to travel back into the computational domain. The boundary conditions can be of different order, where a high order is equivalent with high order derivatives in the PDEs governing the boundary condition. When using such boundary conditions in numerical computations some possible drawbacks become apparent. The first is the question of how to discretize the high order (mixed) derivatives in a stable fashion. A way to handle this problem is to introduce auxiliary variables such that a system of first order PDEs is solved instead of the high order PDE on the boundary. However the issue of a stable discretization may still be present, especially when using numerical methods of high order. The second possible drawback relates to the fact that when any discretization procedure is used, spurious non-physical solutions are introduced. Boundary conditions which are non-reflecting for physical solutions may be highly reflective for its spurious counterpart. This indicates that it may be fruitful to consider *discretely* non-reflecting boundary conditions i.e. boundary conditions which are non-reflecting for both physical and spurious solutions.

The construction of a discretely non-reflecting boundary condition depends on the discretization procedure used, i.e. for each specific scheme a new boundary condition must be derived. In this paper we present the construction of a discretely non-reflecting boundary condition for the one-way wave equation where the standard five-point central difference approximation is used for the first order derivative in space.

In the recent paper [14] Rowley and Colonius have provided a framework for such construction. They construct boundary conditions for an implicit Padé three-point central difference scheme to illustrate their analysis. The discrete boundary conditions are then used to construct boundary conditions for the linearized Euler equations in two dimensions.

We consider a simpler model problem for the extension of our discrete scalar boundary condition to systems in two dimensions. The ideas presented here are

directly applicable to any hyperbolic problem in two dimensions.

The Padé scheme, used in [14], is a fourth order implicit scheme. Widening the stencil from three to five points allows for an explicit fourth order scheme. However the issue of stability of the boundary condition becomes more involved.

The boundary conditions is extended to two space dimensions by combining exact continuous non-reflecting boundary conditions and the one dimensional discretely non-reflecting boundary condition. The resulting boundary condition is localized by the standard Padé approximation. By using auxiliary variables the two dimensional boundary condition can, in principal, be extended to high-order. However it is found by numerical experiments that the resulting method suffers from *boundary instabilities*.

Analysis of a related continuous problem suggests that the discrete boundary condition can be stabilized by adding tangential viscosity at the boundary. For the lowest order Padé approximation we are able to stabilize the discrete boundary condition. However, the results of the stabilized boundary condition is not satisfactory. The reflections are smaller than for the standard boundary condition but does not motivate the extra work needed to implement them.

## 2 Discretely Non-Reflecting Boundary Conditions in one Dimension

When solving hyperbolic problems with numerical methods, it is preferred to use explicit methods both in time and space. For truncated problems, the geometries of the outer boundary can often be chosen as preferred, e.g. as a box. For such simple geometry, the obvious choice of discretization is centered differences of high order in space combined with an explicit high order method (e.g. Runge-Kutta) in time. This combination yields an easy to implement, accurate and fast numerical method. By using centered differences in space and assuming that the grid is regular, at least close to the boundary, the errors produced by spurious waves may be controlled and minimized by discrete analysis.

In section 2.1 we recall some basic facts of finite difference schemes for hyperbolic problems. The notation of physical and spurious waves are introduced together with the discrete group and phase velocity.

In sections 2.2-2.3 we construct approximate discretely non-reflecting boundary conditions such that reflections caused by the coupling of spurious and physical modes are minimized.

### 2.1 Spurious and Physical Waves in One Dimensional Finite Difference Schemes

We begin by considering the scalar one-way wave equation

$$u_t + u_x = 0, \tag{1}$$

which admits solutions on the form

$$u(x, t) = e^{i(kx - \omega t)}. \quad (2)$$

Inserting (2) into (1), we obtain the **dispersion relation**  $\omega \equiv \omega(k) = k$ , where  $k$  is the wave number and  $\omega$  the frequency. For an equation with a dispersion relation, the **phase velocity**,  $c_p$ , and **group velocity**,  $c_g$  can be defined as

$$c_p = \frac{\omega(k)}{k}, \quad c_g = \frac{d\omega(k)}{dk}.$$

For the equation (1),  $c_p = c_g = 1$ .

### Discrete Dispersion Relation

It is well known (see [16] for a detailed discussion) that a discretization of (1) will affect the dispersion relation and thereby the phase and group velocity. Different schemes have different dispersion relations and therefore they have to be analyzed separately.

In [14], Colonus and Rowley analyze a fourth order accurate, compact centered three point difference scheme. The advantage of using a compact three point scheme is that only one type of spurious waves will appear. The main disadvantage is that the scheme is implicit. Here, we will analyze the standard centered five point difference scheme of order four.

We start by introducing a regular grid in  $x$ , with mesh spacing  $h$ . Let  $u_k$  denote the approximation of  $u(x_k)$  where  $x_k = kh$  and  $k = 0, 1, \dots, N$ . We use the central finite difference approximation

$$\frac{\partial u(x_k)}{\partial x} \approx \frac{1}{12h} (-u_{k+2} + 8u_{k+1} - 8u_{k-1} + u_{k-2}). \quad (3)$$

of  $u_x$  in(1) and obtain

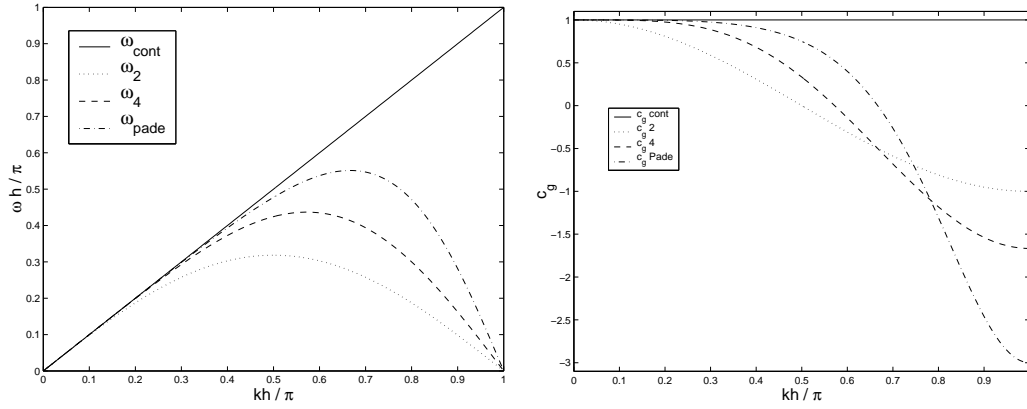
$$(u_t)_k = \frac{1}{12h} (u_{k+2} - 8u_{k+1} + 8u_{k-1} - u_{k-2}). \quad (4)$$

The dispersion relation of (4) is

$$\omega(k) = \frac{4}{3h} \sin kh - \frac{1}{6h} \sin 2kh$$

In Figure 1 we compare dispersion relations and group velocities for the continuous problem and the discretized problem. Note that poorly resolved waves ( $kh \approx \pi$ ) travel in the opposite direction, i.e.  $c_g < 0$ , to well resolved waves.

In Figure 1 (a) we can also see that for each frequency  $\omega(k)$ , there are two values of  $k$  that satisfy the dispersion relation. The smaller one corresponds to a **physical** wave and the larger one corresponds to a **spurious** wave. For three point schemes, these two waves are the only type of waves that exist but for the fourth order scheme



(a) Dispersion relations for different discretizations.

(b) Group velocities for different discretizations.

**Figure 1.** The notation  $\omega_{cont}$ ,  $\omega_2$ ,  $\omega_4$  and  $\omega_{Pade}$  refers to the continuous, standard 2nd order centered scheme, standard 4th order scheme and the compact scheme [14].

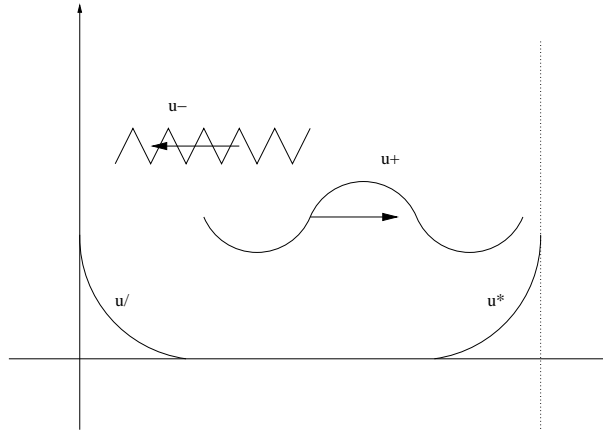


**Figure 2.** Different types of waves supported by standard five point centered difference scheme.  $u^+$  corresponds to a physical right-going wave,  $u^-$  to a spurious left-going wave,  $u^*$  to a spurious wave decaying from the left and  $u^{\dagger}$  to a spurious wave decaying from the right.

(3), there exist four values of  $k$  that satisfies the dispersion relation, see section 2.2. Of these four, two correspond to wave solutions and two to damped wave solutions. This is illustrated in Figure 2.1. The two damped solutions are important for the stability but not for the non-reflectivity of the boundary condition. In short, stability of the boundary condition depends on whether they are uniquely determined.

## 2.2 Separation of Spurious and Physical Modes

By introducing a normal mode solution

$$u_k(t) = \hat{u}e^{i\omega t}\kappa^k,$$

with the property

$$u_{k+1} = \kappa u_k,$$

we obtain the characteristic equation of (4)

$$N(i\omega, \kappa) \equiv [\kappa^4 - 8\kappa^3 - i12\omega h\kappa^2 + 8\kappa - 1] = 0.$$

This equation has four nontrivial solutions

$$\begin{aligned}\kappa^+ &= 2 + \frac{1}{2}\xi - \frac{1}{2}\sqrt{\gamma + \theta}, & \kappa^- &= 2 - \frac{1}{2}\xi - \frac{1}{2}\sqrt{\gamma - \theta}, \\ \kappa^* &= 2 + \frac{1}{2}\xi + \frac{1}{2}\sqrt{\gamma + \theta}, & \kappa^\dagger &= 2 - \frac{1}{2}\xi + \frac{1}{2}\sqrt{\gamma - \theta}.\end{aligned}$$

Here

$$\begin{aligned}\eta &= (-18I\phi + 8I\phi^3 + \sqrt{-125 - 24\phi^2 + 48\phi^4})^{1/3}, \\ \xi &= \sqrt{16 + 8I\phi + (180 - 144\phi^2)/(18\eta) + 2\eta}, \\ \gamma &= 32 + 16I\phi - (180 - 144\phi^2)/(18\eta) - 2\eta, \\ \theta &= (448 + 384I\phi)/(4\xi), \\ \phi &= \omega h, \quad I = \sqrt{-1}.\end{aligned}$$

In order to distinguish the physical part of the solution from the spurious part we write the solution  $u_k$  at a grid-point  $k$  as

$$u_k = u_k^+ + u_k^- + u_k^* + u_k^\dagger,$$

where  $u_k^{\textcircled{a}}$  are normal modes that satisfy

$$N(i\omega, \kappa^{\textcircled{a}})u^{\textcircled{a}} = 0, \quad \textcircled{a} = \{+, -, *, \dagger\}.$$

The solutions  $u^+$  and  $u^-$  denote the physical and the spurious wave while  $u^*$  and  $u^\dagger$  are damped waves that decay from the right and left boundary respectively.

### 2.3 Approximate Non-Reflecting Boundary Conditions

We now seek approximate non-reflecting boundary conditions at the left ( $k = 0$ ) and at the right ( $k = N$ ) boundary. Following the ideas of Coloniuss [2] and Coloniuss and Rowley [14] we seek approximate boundary conditions of the form

$$\frac{du_0}{dt} = \frac{1}{c_1 h} \sum_{k=0}^{N_d} d_k u_k \equiv d_0^i u_0, \quad \frac{du_N}{dt} = \frac{1}{a_1 h} \sum_{k=0}^{N_d} b_k u_{N-k} \equiv d_N^o u_N, \quad (5)$$

where  $a_1, b_k, c_1, d_k, (k = 0, \dots, N_d)$  are coefficients to be determined. Here  $N_d$  is the order of the boundary condition. Consider first the left boundary.

Taking the Fourier transform in time and splitting  $u$  into its different modes, (5) becomes

$$\begin{aligned} ic_1 \omega h (u_0^+ + u_0^- + u_0^* + u_0^\div) &= \sum_{k=0}^{N_d} d_k (u_k^+ + u_k^- + u_k^* + u_k^\div) \\ &\iff ic_1 \omega h u_0^+ - \sum_{k=0}^{N_d} d_k (\kappa^+)^k u_0^+ = \\ &-ic_1 \omega h (u_0^- + u_0^* + u_0^\div) + \sum_{k=0}^{N_d} d_k \left[ (\kappa^-)^k u_0^- + (\kappa^*)^k u_0^* + (\kappa^\div)^k u_0^\div \right]. \end{aligned} \quad (6)$$

With  $\phi = \omega h$ , (6) becomes

$$d^+(\phi) u_0^+ = d^-(\phi) u_0^- + d^*(\phi) u_0^* + d^\div(\phi) u_0^\div,$$

where

$$\begin{aligned} d^+(\phi) &= c_1 i \phi - \sum_{k=0}^{N_d} d_k (\kappa^+)^k, \\ d^\circledast(\phi) &= -c_1 i \phi + \sum_{k=0}^{N_d} d_k (\kappa^\circledast)^k, \quad \circledast = \{-, *, \div\}. \end{aligned}$$

The exact non-reflecting boundary condition,  $u_0^+ = 0$ , would be satisfied if

$$d^\circledast(\phi) = 0, \quad \circledast = \{-, *, \div\}.$$

It is not possible to fulfill  $d^\circledast(\phi) = 0$  for all  $\circledast = \{-, *, \div\}$ . However this is not necessary since  $u^\div$  will be eliminated later and  $u^*$  must be specified at the right boundary and will be very small at the left boundary. Thus only  $d^-(\phi) = 0$  remains, this is equivalent with the condition obtained in [14].

Since  $d^-(\phi)$  contains powers of  $\kappa^-$  up to order  $N_d$ , it is natural to expand  $\kappa^-(\phi)$  as a power series expansion around  $\phi = 0$ . The coefficients  $c_1, d_0, \dots$  are chosen such that  $d^-(\phi)$  is minimized.

At the right boundary we use the same technique to find the boundary condition for  $u_N$ . Separating the spurious and physical modes of the ansatz (5) leads to the following expression

$$b^+(\phi)u_N^+ = b^-(\phi)u_N^- + b^*(\phi)u_N^* + b^\div(\phi)u_N^\div,$$

where

$$b^+(\phi) = ac_1 i\phi - \sum_{k=0}^{N_d} \frac{b_k}{(\kappa^+)^k},$$

$$b^\circledast(\phi) = -a_1 i\phi + \sum_{k=0}^{N_d} \frac{b_k}{(\kappa^\circledast)^k}, \quad \circledast = \{-, *, \div\}.$$

The non-reflecting boundary condition for  $u_N$  is  $b^+(\phi) = 0$ . For an equation with a left-going physical solution, e.g  $v_t - v_x = 0$ , the analysis is similar. The role of the spurious and physical solution at a boundary will be the opposite compared to an equation with a right-going physical solution. Using the notation introduced in (5), we may write boundary closures for the equation  $v_t - v_x = 0$  as

$$\frac{dv_0}{dx} = d_0^o v_0, \quad \frac{dv_N}{dx} = d_N^i v_N.$$

## 2.4 Stability

When applying the scheme (3) to the gridpoint  $k = 1$  we need information of both  $u_0$  and  $u_{-1}$ . Above,  $u_0$  has been determined to minimize the reflection at  $k = 0$ . The relation determining  $u_{-1}$  must be chosen such that the boundary condition is stable. The mathematically correct boundary condition is  $u(t, 0) = 0$ , which together with (1) gives the relation  $u(t, 0)_{xx} = 0$ . First consider a three point wide stencil for the approximation of  $(u_{xx})_{k=0}$ , which yield the relation

$$u_{-1} = 2u_0 - u_1. \quad (7)$$

It can be shown that (7) yields a stable boundary condition for choices of  $N_d$  at least up to  $N_d = 8$ . For example, consider  $N_d = 1$  which gives the following relation for  $u_0$

$$\frac{du_0}{dt} = -\frac{5}{3h}(u_0 + u_1). \quad (8)$$

To investigate the stability of the above boundary conditions for (4) we use Laplace transform technique (see e.g. [9]). We obtain the following eigenvalue problem

$$\tilde{s}\psi_j = \frac{1}{12h}(\psi_{j+2} - 8\psi_{j+1} + 8\psi_{j-1} - \psi_{j-2}), \quad \tilde{s} = sh. \quad (9)$$

There are two roots,  $\kappa_\nu$ ,  $\nu = 1, 2$ , to the characteristic equation associated with (9), with  $|\kappa_\nu| \leq 1$  for  $\text{Re } \tilde{s} > 0$ . The general solution of (9) with  $\|\psi\|_h < \infty$  has the form

$$\psi_j = \sigma_1 \kappa_1^j + \sigma_2 \kappa_2^j, \quad \text{if } \kappa_1 \neq \kappa_2, \quad (10)$$

$$\psi_j = \sigma_1 \kappa_1^j + \sigma_2 j \kappa_1^{j-1}, \quad \text{if } \kappa_1 = \kappa_2. \quad (11)$$

First consider the case  $\kappa_1 \neq \kappa_2$ . Inserting the general solution (10) into the boundary conditions (7) and (8), we obtain the following equations for  $\sigma_1$  and  $\sigma_2$

$$\begin{aligned} \frac{\sigma_1}{\kappa_1} + \frac{\sigma_2}{\kappa_2} &= 2\sigma_1 + 2\sigma_2 - \kappa_1 \sigma_1 - \kappa_2 \sigma_2, \\ \tilde{s}(\sigma_1 + \sigma_2) &= \frac{5}{3}(-\sigma_1 - \sigma_2 - \kappa_1 \sigma_1 - \kappa_2 \sigma_2), \end{aligned}$$

which may be formulated as a linear system of equations  $C(\tilde{s}, \kappa_1, \kappa_2)\sigma = 0$ . A necessary and sufficient condition for stability is that  $\det C \neq 0$  for all  $\text{Re } s \geq 0$ . The determinant of  $C$  is

$$\det C = \frac{(\kappa_1 - \kappa_2)(15\kappa_2\kappa_1 - 5\kappa_1 + 3\kappa_1\tilde{s}\kappa_2 - 5 - 3\tilde{s} - 5\kappa_2)}{3\kappa_2\kappa_1}$$

Clearly the first factor cannot be zero since  $\kappa_1 \neq \kappa_2$ . Assuming that the second factor is zero we solve for  $\tilde{s}$

$$\tilde{s} = -\frac{5(1 + \kappa_1 + \kappa_2 - 3\kappa_1\kappa_2)}{3(1 - \kappa_2\kappa_1)}.$$

We want to show that there is no solutions  $\text{Re } s \geq 0$ . The the real part of the denominator is always positive except when  $\kappa_1 = \kappa_2 = \pm 1$  which would be a contradiction to the assumption  $\kappa_1 \neq \kappa_2$ . By similar arguments arguments the real part of the numerator must always be positive. Hence, there are no solutions with  $\text{Re } s \geq 0$  if  $\kappa_1 \neq \kappa_2$ .

Now consider the case  $\kappa_1 = \kappa_2$ . Inserting the general solution (11) into the boundary conditions (7) and (8) yields the determinant

$$\det C = \frac{-(3s\kappa_1^2 - 3s + 15\kappa_1^2 - 5 - 10\kappa_1)}{3\kappa_1^2} \equiv \frac{p_1(\kappa)}{3\kappa_1^2}.$$

The characteristic equation determining the root  $\kappa_1$  is

$$p_2(\kappa) \equiv \kappa_1^4 - 8\kappa_1^3 - 12s\kappa_1^2 + 8\kappa_1 - 1.$$

If there is no solution to the system

$$\begin{aligned} p_1(\kappa) &= 0 \\ p_2(\kappa) &= 0 \end{aligned} \quad (12)$$

the boundary conditions are stable. The problem to determine if such solutions exist is known as the consistency problem and can be solved using Gröbner basis

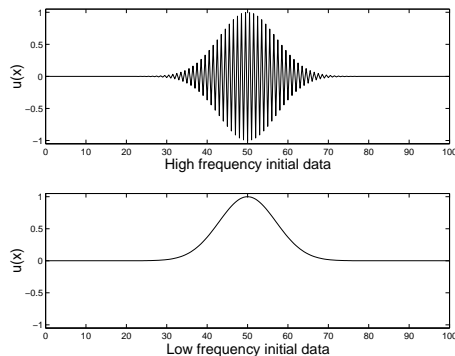


**Figure 3.** Initial data for experiments in one dimension.

[3]. Using the symbolic software Maple we are able to determine that there are no solutions to the system (12), hence the boundary conditions are stable.

Note that the boundary condition (7) is only second order which would degrade the overall accuracy of the method if used. Instead of (7) we use the fourth order accurate, five point, skew approximation of  $u_{xx}$  which also will yield a stable boundary condition. Since this approximation is used, the overall order of the method will be four.

For the right boundary, a skew difference stencil  $D_-^q u_{N-1}$  together with the non-reflective boundary conditions derived above can be shown to yield a stable boundary condition. If  $q$  is chosen large enough the overall order of accuracy will be four.

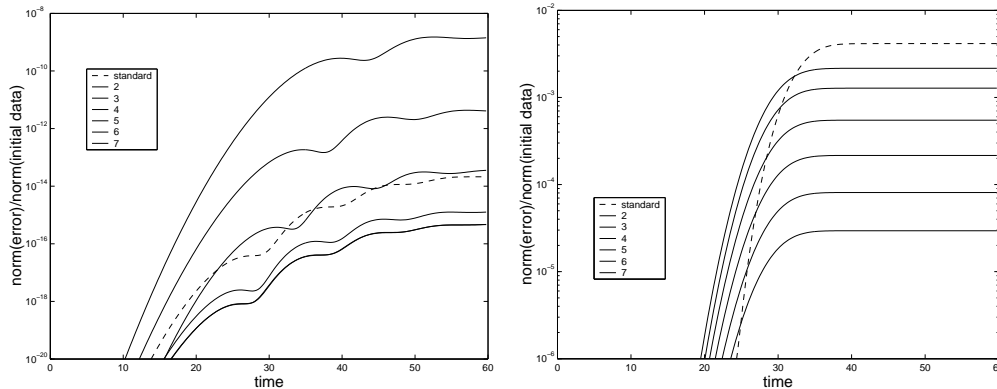
## 2.5 Numerical experiments in 1D

To test the boundary condition, we consider the one-way wave equation (1) on the computational domain  $x \in [0, 100]$ , discretized with a regular grid. The spatial derivative is approximated by using the fourth order stencil (3) terminated using the discretely non-reflecting boundary conditions discussed in the previous section. The integration in time is performed with the standard fourth order Runge Kutta method. As a comparison, we use characteristic boundary conditions, i.e.  $u(0, t) = 0$ , together with extrapolation at the right boundary. The error is computed using a reference solution computed on a larger domain.

The boundary conditions are tested for two sets of initial data  $u(x, 0)$

$$\begin{aligned} u_{\text{high}}(x_k) &= (-1)^k u(x_k), \\ u_{\text{low}}(x_k) &= u(x_k), \\ u(x) &= e^{-\frac{(x-50)^2}{10^2}}. \end{aligned}$$

The initial data  $u_{\text{high}}$  is oscillating with the highest frequency allowed on the grid while the initial data  $u_{\text{low}}$  is smooth, see Figure 3. In Figure 4 the error for different



(a) The  $l_2$  error on the computational domain for the smooth initial data for different  $N_d$  compared with characteristic boundary conditions. For  $N_d > 4$  the discretely non-reflecting boundary condition outperforms the characteristic boundary condition.

(b) The  $l_2$  error on the computational domain for the non-smooth initial data for different  $N_d$  compared with characteristic boundary conditions. Here the discretely non-reflecting boundary condition is more efficient than characteristic boundary conditions for all  $N_d$ .

**Figure 4.**

$N_d$  is compared to the error introduced by characteristic boundary conditions. It is clear that for large  $N_d$ , the discretely non-reflecting boundary conditions are more efficient than characteristic boundary conditions independent of the smoothness of the initial data. Especially for the non-smooth initial data, the discretely non-reflecting boundary condition works well.

### 3 Continuous Non-Reflecting Boundary Conditions

An important feature of linear systems of hyperbolic equations is that it is possible to separate in-going and out-going parts of the solution at a boundary. The decomposition of the solution at a boundary is obtained by using the theory of characteristics. This decomposition of the solution is closely related to the well-posedness of the problem. The necessary condition for well-posedness is that in-going components of the solution must be specified by the boundary conditions at each boundary.

If the boundary condition is to be well-posed and non-reflecting, the in-going modes should be put to zero. This will prevent reflection of the solution back into the domain. Below, we construct well-posed, non-reflecting boundary conditions for a simple model problem in two dimensions. For a complete discussion of construction

of continuous non-reflecting boundary conditions for linear hyperbolic systems see [14] or [6].

### 3.1 A Model Problem in 2D

Consider the system

$$w_t + Aw_x + Bw_y = 0, \quad (13)$$

on the domain  $0 \leq x \leq L$ ,  $-\infty < y < \infty$ ,  $t > 0$ , where

$$w = \begin{bmatrix} u \\ v \end{bmatrix}, \quad A = \begin{bmatrix} 1 & 0 \\ 0 & -1 \end{bmatrix}, \quad B = \begin{bmatrix} 0 & 1 \\ 1 & 0 \end{bmatrix}.$$

To derive non-reflecting boundary conditions for (13) at  $x = 0$  and  $x = L$ , we take the Laplace transform in time and the Fourier transform in the  $y$  direction. The transformed system is

$$\hat{w}_x = -A^{-1}(sI + ikB)\hat{w},$$

where  $(s, k)$  are the duals of  $(t, y)$ . Let  $z = ik/s$ , then we may write

$$\hat{w}_x = -sA^{-1}(I + zB)\hat{w} \equiv -sM(z)\hat{w}. \quad (14)$$

Since (13) is a hyperbolic problem, we can decompose the solution into left and right-going waves. The right-going waves are those corresponding to positive eigenvalues of  $M(z)$  at  $z = 0$  and the left-going those that correspond to negative eigenvalues.

The eigenvalues and left eigenvectors of  $M(z)$  are (here the subscript R denotes right-going and L denotes left-going waves)

$$\begin{aligned} \lambda_R &= \sqrt{1 - z^2}, & Q_R &= \begin{bmatrix} 1 + \sqrt{1 - z^2} \\ z \end{bmatrix}^T, \\ \lambda_L &= -\sqrt{1 - z^2}, & Q_L &= \begin{bmatrix} 1 - \sqrt{1 - z^2} \\ z \end{bmatrix}^T. \end{aligned}$$

Using the diagonalization

$$QMQ^{-1} = \begin{bmatrix} \lambda_R & 0 \\ 0 & \lambda_L \end{bmatrix},$$

where

$$Q = \begin{bmatrix} Q_R \\ Q_L \end{bmatrix},$$

to decouple the system (14) into two scalar equations, it is easy to see that the exact non-reflecting boundary conditions for (13) are

$$\begin{aligned} Q_R \hat{w} &= 0 \quad \text{at } x = 0, \\ Q_L \hat{w} &= 0 \quad \text{at } x = L. \end{aligned} \quad (15)$$

The exact non-reflecting boundary condition (15) contains the non-rational function  $\sqrt{1 - z^2}$ , which does not have an explicit inverse transform. Consequently, the

corresponding boundary condition in the physical space will be exact but nonlocal in time and space. This non locality is undesirable and leads to expensive and cumbersome implementation of the boundary conditions when used for computations. To localize these boundary conditions,  $\sqrt{1 - z^2}$  may e.g. be replaced by some rational approximant, which can be transformed back directly.

### 3.2 Rational Approximants and Non-Reflecting Boundary Conditions

The problem of approximating the function  $\sqrt{1 - z^2}$  in the context of non-reflecting boundary conditions has been extensively studied in the literature. See e.g. Engquist and Majda [4]. Trefethen and Halpern [15] provides detailed studies of different type of approximations (Padé, Chebyshev and least-squares).

In this paper we consider only the Padé approximations which yield well-posed, see [15], boundary conditions in exactly the diagonals,  $m = n$  and  $m = n + 2$  of the table of approximants  $(m, n)$ .

By replacing  $\sqrt{1 - z^2}$  with the Padé approximant, in  $Q_R$  and  $Q_L$ , we obtain the following approximate non-reflecting boundary conditions

$$\begin{aligned} E_R \hat{w} &= 0 \text{ at } x = 0, \\ E_L \hat{w} &= 0 \text{ at } x = L. \end{aligned} \tag{16}$$

## 4 Discretely Non-Reflecting Boundary Conditions in 2D

To derive a discretely non-reflecting boundary condition in two dimensions, we can use the exact boundary conditions, discussed in section 3.1, together with the discretely non-reflecting boundary conditions discussed in section 2.3. Since the discretely non-reflecting boundary conditions are directly applicable for one-way equations we use the exact continuous boundary conditions for (13) to obtain one-way equations.

Consider again the transformed version of the system (13)

$$\hat{w}_x = -sM(z)\hat{w}, \tag{17}$$

with the exact non-reflecting boundary conditions (15)

$$\begin{aligned} Q_R \hat{w} &= 0 \text{ at } x = 0, \\ Q_L \hat{w} &= 0 \text{ at } x = L. \end{aligned}$$

Now define the matrix

$$Q(z) = \begin{bmatrix} Q_R \\ Q_L \end{bmatrix},$$

and let  $T(z)$  be the matrix composed by the right eigenvectors to  $M(z)$  such that

$$T^{-1}MT = \begin{bmatrix} \lambda_R & 0 \\ 0 & \lambda_L \end{bmatrix} \equiv \Lambda. \tag{18}$$

The matrix  $C = QT$  is diagonal and invertible since the boundary conditions are well posed. Hence,  $Q$  is also invertible and we may use the transformation  $g = Q\hat{w}$  in (17) with the result

$$\begin{aligned}\frac{d}{dx}Q\hat{w} &= -s(QMe^{-1})Q\hat{w} \Rightarrow \\ \frac{d}{dx}g &= -s\Lambda g.\end{aligned}$$

We obtain two decoupled one way equations

$$\frac{d}{dx}g^R = -s\lambda_R g^R, \quad \frac{d}{dx}g^L = -s\lambda_L g^L.$$

Introduce a regular grid in  $x$ , with mesh spacing  $h$ , and let  $g_k$  denote the approximation of  $g(x_k)$  at  $x_k = kh$ ,  $k = 0, 1, \dots, N$ . The discrete non-reflecting boundary conditions at the left and right boundary, respectively, are

$$\begin{aligned}d_0^i g_0^R &= -s\lambda_R g_0^R, & d_0^o g_0^L &= -s\lambda_L g_0^L, \\ d_N^i g_N^R &= -s\lambda_R g_N^R, & d_N^o g_N^L &= -s\lambda_L g_N^L.\end{aligned}$$

Defining

$$D_L = \begin{bmatrix} d_0^i & 0 \\ 0 & d_0^o \end{bmatrix}, \quad D_R = \begin{bmatrix} d_N^o & 0 \\ 0 & d_N^i \end{bmatrix},$$

and transforming back to  $\hat{w}$ , we obtain the boundary conditions

$$\begin{aligned}-sQ(z)M(z)\hat{w}_0 &= D_L Q(z)\hat{w}_0, \\ -sQ(z)M(z)\hat{w}_N &= D_R Q(z)\hat{w}_N.\end{aligned}\tag{19}$$

The boundary conditions (19) need to be transformed back to the physical space to be useful. Since  $Q(z)$  contains non-rational functions of  $z$ , this will lead to boundary conditions which are nonlocal both in time and space. By replacing  $Q(z)$  by a rational approximant  $E(z)$ , as described in section 3.2, the boundary conditions (19) become

$$\begin{aligned}E(z)\frac{\hat{w}_0}{dx} &= D_L E(z)\hat{w}_0, \\ E(z)\frac{\hat{w}_N}{dx} &= D_R E(z)\hat{w}_N.\end{aligned}\tag{20}$$

Here we have used the interior equations (17). Since  $E(z)$  is a rational function (20) can be transformed to a local boundary condition by inverse Laplace and Fourier transform.

Using a high order approximant in the construction of  $E(z)$  will result in a boundary condition containing high order mixed derivatives in  $t$  and  $y$ . In general high order derivatives are undesirable since they are difficult to discretize in a stable

and accurate manner. Especially, this is true when using a high order scheme in the interior.

To obtain boundary conditions containing no mixed derivatives, auxiliary variables may be introduced. These variables can be chosen in many ways. Here we chose the approach suggested in Rowley and Colonius [14]. Alternative approaches can be found in e.g. Hagstrom and Harihan [8] or Givoli and Neta [7].

#### 4.1 Non-Reflecting Boundary Conditions using Auxiliary Variables

We start by multiplying each row of equation (20) by its least common denominator to obtain the following system

$$E'(z) \frac{\hat{w}_0}{dx} = D_L E'(z) \hat{w}_0, \quad (21)$$

$$E'(z) \frac{\hat{w}_N}{dx} = D_R E'(z) \hat{w}_N, \quad (22)$$

where

$$E'(z) = E_0 + zE_1 + \dots + z^p E_p.$$

Introduce auxiliary variables  $h_j$  such that (21) becomes

$$\begin{aligned} E_0 \frac{\partial w_0}{\partial x} &= D_L E_0 w_0 + \frac{\partial}{\partial y} (F_0 w_0 + h_1), \\ \frac{\partial h_j}{\partial t} &= D_L E_j w_0 + \frac{\partial}{\partial y} (F_j w_0 + h_{j+1}), \quad j = 1, \dots, p-1 \\ \frac{\partial h_p}{\partial t} &= D_L E_p w_0 + \frac{\partial}{\partial y} (F_p w_0), \end{aligned} \quad (23)$$

where

$$\begin{aligned} F_0 &= E_1 A^{-1}, \\ F_j &= E_j A^{-1} B + E_{j+1} A^{-1}, \quad j = 1, \dots, p-1 \\ F_p &= E_p A^{-1} B. \end{aligned}$$

The boundary condition (23) is easy to implement and the extra amount of memory needed for the auxiliary variables is proportional to the order of the rational approximant. For the boundary conditions at the right boundary, simply replace  $w_0$  by  $w_N$ .

## 4.2 Stability of the Non-Reflecting Boundary Conditions

Consider (23) with the Pade expansion (0,0) and  $N_d = 2$  for the operators  $d_0^i$  and  $d_0^o$ . For these choices, (23) become

$$\begin{aligned}\frac{\partial u_0}{\partial x} &= d_0^i u_0 + \frac{1}{2} \frac{\partial}{\partial y} (-v_0 + h_1), \\ \frac{\partial v_0}{\partial x} &= d_0^o v_0 \\ \frac{\partial h_1}{\partial t} &= d_0^i v_0\end{aligned}\tag{24}$$

with

$$d_0^i q_0 = \frac{3}{5h} (q_0 + q_1), \quad d_0^o q_0 = \frac{1}{h} (-q_0 + q_1).$$

In the gridpoints next to the boundary a skew approximations for the x-derivatives of  $u$  and  $v$  are used. When approximating  $u_x$ ,  $\tilde{d}^i$  is used and when approximating  $v_x$ ,  $\tilde{d}^o$  is used. The skew operators are chosen as

$$\tilde{d}^i q_1 = \frac{1}{12h} (-6q_0 - q_1 + 8q_2 - q_3), \quad \tilde{d}^o q_1 = \frac{1}{h} (q_2 - q_1).\tag{25}$$

When we solve (13) numerically, using these boundary conditions at  $x = 0$  and periodic boundary conditions in  $y$  we experience instability. The instability appear at  $x = 0$ . The unstable solution is highly oscillatory in  $y$  and decay rapidly into the computational domain. The decay and the oscillations indicated that the instabilities are so called *boundary instabilities* [12]. To further investigate this problem, we analyze a continuous model problem.

## 4.3 Stability of a Model Problem

By investigating the well-posedness of a continuous model problem, similar in structure to (24), we hope to identify the mechanisms responsible for the instability of the non-reflecting boundary conditions (24). The problem we consider is equation (13) with initial data  $w(0, x, y) = f(x, y)$  on the domain  $\{0 \leq x < \infty, -\infty < y < \infty, t > 0\}$  closed with the boundary condition

$$u_x = -(u + 2u_t + u_y - \varepsilon u_{yy}), \quad \varepsilon \geq 0.\tag{26}$$

We will use the Laplace transform technique [11] to determine the well-posedness of the stated problem. The problem (13), (26) is said to be ill-posed in any sense if there exist a solution

$$w = e^{st+iky} \Psi(x), \quad \text{Re } s > 0, \|\Psi(x)\| < \infty, k \text{ real.}$$

For the problem (13), (26) we have the following lemma.

**Lemma 1** *The problem (13), (26) is ill-posed for  $\varepsilon = 0$  and well-posed for  $\varepsilon > \frac{4+\sqrt{106}}{45}$ .*

**Proof of Lemma 1** Inserting the ansatz  $w = e^{st+iky}\Psi(x)$  into (13) yields the eigenvalue problem

$$(sI + ikB)\Psi + A\Psi_x = 0, \quad (27)$$

with the eigenvalues  $\lambda_1 = -\lambda_2 = -\sqrt{s^2 + k^2}$ . The solution of (27) satisfying  $\|\Psi(x)\| < \infty$  is

$$\Psi(x) = \sigma e^{-\sqrt{s^2+k^2}x}\Phi. \quad (28)$$

Here  $\Phi = [\phi_1, \phi_2]^T = [-s\sqrt{s^2+k^2}, ik]^T$  is the eigenvector corresponding to  $\lambda_1$ . To be a solution, (28) must fulfill the boundary condition (26). This leads to the algebraic relation

$$-\sqrt{s^2+k^2} = -(1+2s+ik+\varepsilon k^2), \quad (29)$$

which must hold for  $\sigma \neq 0$ . By solving explicitly for  $s$

$$s = -\frac{2(1+\varepsilon k^2)}{3} - \frac{i2k}{3} + \frac{1}{3}\sqrt{1+2\varepsilon k^2+i2k+\varepsilon^2 k^4+i2k^3\varepsilon+2k^2}.$$

For  $\varepsilon = 0$  we have

$$s = -\frac{2}{3} - \frac{i2k}{3} + \frac{1}{3}\sqrt{1+i2k+2k^2}.$$

For  $k = 0$  we have  $\text{Re } s = -2/3$  so the problem is well posed for data which does not vary in the  $y$ -direction. However, for large  $k$ ,  $\text{Re } s \sim k$  and we conclude that there exist some  $k_0$  such that the problem is ill-posed for all  $k > k_0$ . For  $\varepsilon > 0$  a sufficient condition for well-posedness is that

$$2(1+\varepsilon k^2) > |\sqrt{1+2\varepsilon k^2+i2k+\varepsilon^2 k^4+i2k^3\varepsilon+2k^2}| = \\ ((1+2k^2(1+\varepsilon)+\varepsilon^2 k^4)^2 + (2k+2k^3\varepsilon)^2)^{1/4}$$

Taking both sides raised to the fourth power gives

$$16 + 64\varepsilon k^2 + 96\varepsilon^2 k^4 + 64\varepsilon^3 k^6 + 16\varepsilon^4 k^8 > \\ 1 + (8+4\varepsilon)k^2 + (2\varepsilon^2 + (2+2\varepsilon)^2 + 8\varepsilon)k^4 + (2(2+2\varepsilon)\varepsilon^2 + 4\varepsilon^2)k^6 + \varepsilon^4 k^8. \quad (30)$$

By inspection of the coefficients it is clear that (30) hold if  $\varepsilon > \frac{4+\sqrt{106}}{45}$ .  $\square$

For the case  $\varepsilon = 0$ , the solution will be  $\hat{w} = e^{st+iky-\sqrt{s^2+k^2}x}\Phi$ . This solution grows exponentially in time, oscillates rapidly in the  $y$  direction ( $k$  is large) but decays exponentially in the  $x$  direction. Usually, this kind of instability is referred to as a *boundary instability*. When this type of instability occurs in an numerical

method, the remedy is to add a small number of tangential viscosity to stabilize the numerical method. The addition of tangential viscosity can be understood by the above analysis. Since the boundary condition (26) has a structure similar to the discrete boundary condition (23), it is reasonable to expect that instabilities observed in the numerical computations may be removed by adding a sufficient amount of tangential viscosity.

#### 4.4 Stabilized Non-Reflecting Boundary Condition

We want to add viscosity to stabilize the boundary conditions (24). Viscosity is introduced by adding the term  $\varepsilon v_{yy}$  to the first row of the equations (13). This is equivalent to modify the the matrix  $M(z)$  to

$$\tilde{M}(z) = \begin{bmatrix} 1 + \varepsilon k^2 & z \\ -z & -1 \end{bmatrix}.$$

This modification is used at the two gridpoints next to the boundary.

To analyze the stabilized boundary conditions, we use the Laplace transform technique on the halfplane problem, defined by the equations (13), (24) on  $\{0 \leq x < \infty, -\infty < y < \infty, t > 0\}$ . Taking the Fourier transform in y direction and the Laplace transform in time yield the following relations at the gridpoints  $x_i, i = \{0, 1, 2\}$

$$\begin{aligned} -sE'(z)M(z)\hat{w}_0 &= D_L E'(z)\hat{w}_0, \\ -s\tilde{M}(z)\hat{w}_1 &= \tilde{D}\hat{w}_1, \\ -s\tilde{M}(z)\hat{w}_2 &= D^{(4)}\hat{w}_2. \end{aligned} \tag{31}$$

The first relation contains the non-reflecting boundary condition (24). The second equation contains the operator  $\tilde{D} = \text{diag}(\tilde{d}^i, \tilde{d}^o)$  defined in (25). The operator  $D^{(4)}$  is the usual fourth order accurate approximation of the derivative and the matrix  $\tilde{M}(z)$  is modified as described above.

Away from the boundary, the solution is determined by the equation

$$-sM(z)\hat{w}_k = D^{(4)}\hat{w}_k, \quad k > 2. \tag{32}$$

The general solution of (32), satisfying  $\|\hat{w}_k\|_h < \infty, \forall k$  with  $\text{Re } s > 0$ , is

$$\hat{w}_k = \left[ \sigma_R^+(\kappa_R^+)^k + \sigma_R^{\dot{-}}(\kappa_R^{\dot{-}})^k \right] \Psi_R(z) + \left[ \sigma_L^-(\kappa_L^+)^k + \sigma_L^*(\kappa_L^*)^k \right] \Psi_L(z). \tag{33}$$

Here the  $\sigma_R^+, \sigma_R^{\dot{-}}, \sigma_L^-, \sigma_L^*$  are constants to be determined by the relations (31). The subscript  $L$  correspond to a left-going mode and  $R$  to a right-going. The vectors

$\Psi_L(z)$  and  $\Psi_R(z)$  are the right eigenvectors of the matrix  $M(z)$  corresponding to the eigenvalues  $\lambda_L$  and  $\lambda_R$ . The different  $\kappa$  are the roots to the equations

$$\begin{aligned}\kappa_R^4 - 8\kappa_R^3 + 12hs\sqrt{1-z^2}\kappa_R^2 + 8\kappa_R - 1 &= 0, \\ \kappa_L^4 - 8\kappa_L^3 - 12hs\sqrt{1-z^2}\kappa_L^2 + 8\kappa_L - 1 &= 0,\end{aligned}$$

satisfying  $|\kappa| < 1$ . It is possible to show, see [9], that for  $\text{Re } s > 0$  there exist exactly two solutions with amplitude less than one to each of the above characteristic equations.

Inserting the solution (33) into the boundary conditions at  $x_1$  and  $x_2$  together with the boundary conditions at  $x_0$ , where  $\hat{u}_0$  and  $\hat{v}_0$  are considered as unknowns, yields a system of equations

$$C(\tilde{s}, k) \begin{bmatrix} \hat{u}_0 \\ \hat{v}_0 \\ \sigma_R^+ \\ \sigma_R^- \\ \sigma_L^- \\ \sigma_L^* \end{bmatrix} = 0.$$

Here  $\tilde{s} = sh$  and  $C(\tilde{s}, k)$  is a 6 by 6 complex matrix with elements that are nonlinear in  $\tilde{s}$  and  $k$ .

The numerical method defined by (31) and (32) is unstable if the determinant of  $C(\tilde{s}, k)$  vanishes for any  $(\tilde{s}, k)$  with  $\text{Re } \tilde{s} > 0$ . Due to the nonlinear structure of the elements, we have been unable to find analytic expressions for the zeros of  $\det C(\tilde{s}, k)$ . However, by numerical examination of  $\det C(\tilde{s}, k)$ , we are able to determine if there are any zeros in the right half of the complex  $\tilde{s}$  plane.

First, considering the case  $\varepsilon = 0$  we find a zero which moves as the parameter  $k$  changes. For small  $k$  it will move towards the left halfplane, and for large  $k$  into the right, i.e. the method is stable for small  $k$  but not for large  $k$ . This behavior is similar to that of the model problem. As for the model problem, we add tangential viscosity at the boundary to remove the instability.

In Figure 5 we have plotted the location of the zeros of  $\det C(\tilde{s}, k)$  in the  $\tilde{s}$  plane as a function of  $k$  for different amounts of viscosity. By increasing  $\varepsilon$  we see that the curves move towards the stable left halfplane. Empirical studies show that the amount of viscosity needed, for all zeros in the right halfplane to disappear, is proportional to the stepsize  $h$  with some modest constant.

For boundary conditions using higher order Padé approximations, we have also experienced instabilities which seem to be related to large wavenumber  $k$ . However, we have not been able to remove these instabilities by adding viscosity.

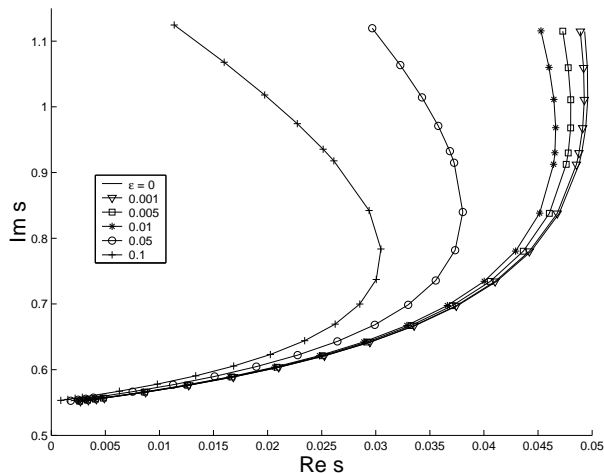


**Figure 5.** The location of the zeros of  $\det C(\tilde{s}, k)$  in the  $\tilde{s}$  plane as a function of  $k$  for different amount of viscosity. The zeros start in the lower left part of the Figure and move along the lines to the right as  $k$  increases.

#### 4.5 Numerical Experiments in 2D

Consider the problem (13) with the initial data

$$w(x, y, 0) = \begin{pmatrix} 1 \\ -1 \end{pmatrix} e^{-\frac{(x-0.5)^2 + (y-0.5)^2}{0.1^2}},$$

on the domain  $(x, y) \in [0, 4] \times [0, 1]$  with periodic boundary conditions in the  $y$  direction and the boundary condition (23) on the left boundary. We only want to consider effects from the left boundary so we choose the placement of the right boundary such that it does not influence the measured error from the left boundary. The error measured is the  $L_2$  error in the domain  $(x, y) \in [0, 0.1] \times [0, 1]$  and is calculated from a reference solution obtained on a larger domain. The results are compared with results obtained when using characteristic boundary conditions, see Figure 6. The boundary condition is better than the characteristic boundary condition for all times. However the increase in performance is small compared with the additional work needed to implement (23).

## 5 Summary

Discretely non-reflecting and stable boundary conditions for hyperbolic systems in one space dimension have been derived. The boundary conditions work well for both spurious and physical waves. The performance increases with the order  $N_d$ .

The boundary conditions is extended to two space dimensions by combining exact continuous non-reflecting boundary conditions and the one dimensional discretely non-reflecting boundary condition. The resulting boundary condition is localized by

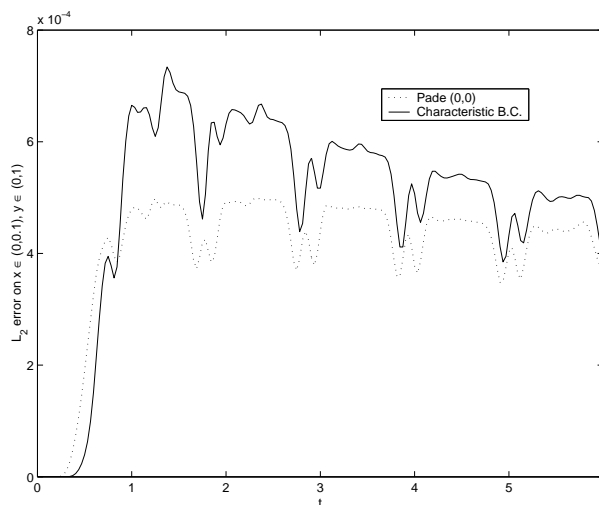


**Figure 6.**

the standard Padé approximation. By using auxiliary variables the two dimensional boundary condition can, in principal, be extended to high-order. However it is found by numerical experiments that the resulting method suffers from *boundary instabilities*. Analysis of a related continuous problem suggests that the discrete boundary condition can be stabilized by adding tangential viscosity at the boundary. For the lowest order Padé approximation we are able to stabilize the discrete boundary condition. However, the results of the stabilized boundary condition is not satisfactory. The reflections are smaller than for the characteristic boundary condition but does not motivate the extra work needed to implement them.

## References

- [1] F. Collino and P.B. Monk, *Optimizing the perfectly matched layer*, Comput. Methods Appl. Energ., pp. 157–171, **164**, (1998).
- [2] T. Colonius, *Numerically nonreflecting boundary and interface conditions for compressible flow and aeroacoustic computations*, AIAA Journal, pp. 1126 **35** (1997).
- [3] D. Cox, J. Little and D. O’Shea, *Ideals, Varieties and Algorithms*, Undergraduate Texts in Mathematics. (Springer-Verlag, New York 1992)
- [4] B. Engquist and A. Majda, *Absorbing boundary conditions for the numerical simulation of waves*, Math. Comp., pp. 629, **31**, (1977).
- [5] B. Engquist and A. Majda, *Radiation Boundary Conditions for Acoustic and Elastic wave Calculations*, Comm. Pure. Appl. Math., pp. 313-357, **32**, (1979).

- [6] M. Giles, *Nonreflecting Boundary Conditions for Euler Equation Calculations*, AIAA Journal, 28:2050-2058, (1990).
- [7] D. Givoli and B. Neta, *High-order non-reflecting boundary scheme for time dependent waves*, J. Comput. Phys., 186 :24-46, (2003).
- [8] J. W. Goodrich and T. Hagstrom, *Accurate Algorithms and Radiation Boundary Conditions for Linearized Euler Equations*, AIAA Paper 96-1600, 1996.
- [9] B. Gustafsson, H-O. Kreiss and J. Olinger, *Time Dependent Problems and Difference Methods*, Pure and Applied Mathematics. (Wiely, New York 1995)
- [10] T. Hagstrom and S.I. Harihan, *A formulation of asymptotic and exact boundary conditions using local operators*, Appl. Numer. Math., pp. 403-416, **27**, (1998).
- [11] H-O. Kreiss and J. Lorenz, *Initial-Boundary Value Problems and the Navier-Stokes Equations*, Pure and Applied Mathematics. (Academic Press, 1989)
- [12] H-O. Kreiss, N. A. Petersson amd J. Ystrom, *Difference approximations for the second order wave equation*, SIAM J. Numer. Anal., 40:1940-1967, (2002).
- [13] E. L. Lindman, *"Free space" Boundary Conditions for the Time Dependent Wave Equation* , J. Comput. Phys., pp. 66-78, **18** (1975).
- [14] C. W. Rowley and T. Colonius, *Discretely Nonreflectiing Boundary Conditions for Linear Hyperbolic Systems*, J. Comput. Phys., pp. 500-538, **157** (2000).
- [15] L.N. Trefethen and L. Halpern, *Well-Posedness of One-Way Wave Equations and Absorbing Boundary Conditions*, Math. Comp., pp. 421-435, **176**, (1986).
- [16] L.N. Trefethen, *Group Velocity in Finite Difference Schemes*, SIAM review, pp. 113-136, **24**, (1982).